ANTIQUITY
a review of world archaeology

CAMBRIDGE
UNIVERSITY PRESS

Origins of Decorated Ostrich Eggs in the Ancient Mediterranean and Middle East

Journal:	*Antiquity*
Manuscript ID	AQY-RE-19-016.R2
Manuscript Type:	Research
Date Submitted by the Author:	n/a
Complete List of Authors:	Hodos, Tamar; University of Bristol, Anthropology and Archaeology Cartwright, Caroline; The British Museum, Department of Scientific Research Montgomery, Janet; Durham University, Department of Archaeology Nowell, Geoff; Durham University, Department of Earth Sciences Crowder, Kayla; Durham University, Department of Archaeology Fletcher, Alexandra; The British Museum, Department of the Middle East Gönster, Yvonne; Deutsches Schloss- und Beschlägemuseum, Wissenschaftliche Mitarbeiterin
Keywords:	ostrich eggs, Mediterranean, Middle East, Bronze and Iron Ages, Isotopes, Scanning Electron Microscopy
Research Region:	Mediterranean Europe

SCHOLARONE™
Manuscripts

Origins of Decorated Ostrich Eggs in the Ancient Mediterranean and Middle East

Tamar Hodos[1,*], Caroline R. Cartwright[2], Janet Montgomery[3], Geoff Nowell[4], Kayla Crowder[3], Alexandra C. Fletcher[5] & Yvonne Gönster[6]

[1] *Department of Anthropology and Archaeology, University of Bristol, 43 Woodland Road, Bristol, BS8 1UU, UK*

[2] *Department of Scientific Research, The British Museum, Great Russell Street, London, WC1B 3DG, UK*

[3] *Department of Archaeology, Durham University, Dawson Building, South Road, Durham, DH1 3LE, UK*

[4] *Department of Earth Sciences, Durham University, Dawson Building, South Road, Durham, DH1 3LE, UK*

[5] *Department of the Middle East, The British Museum, Great Russell Street, London, WC1B 3DG, UK*

[6] *Deutsches Schloss- und Beschlägemuseum, Oststraße 20, 42551 Velbert, Germany*

[*] *Author for correspondence (Email: t.hodos@bristol.ac.uk)*

Decorated ostrich eggs were traded around the Mediterranean during the Bronze and Iron Ages. Research on their origins has focused primarily on decorative techniques and iconography to characterise producers, workshops and trade routes, thereby equating decorative styles with cultural identities and geographical locations. This is problematic for these periods, as craftspeople were mobile and in service to foreign royal patrons. Consequently, the present study investigates geographical origin and reconsiders trade patterns via isotopic indicators. Scanning electron microscopy has also been used to characterise decorative techniques to assist in recognising culturally distinct decorative styles or regional preferences.

Keywords: ostrich eggs, Mediterranean, Middle East, North Africa, Bronze Age, Iron Age, isotopes, SEM

Introduction

Decorated ostrich eggs were produced and traded as luxury items in antiquity. They were engraved, painted, and embellished with ivory, precious metals and faience fittings. They were deposited primarily in elite funerary contexts from Mesopotamia and the Levant to the wider Mediterranean throughout the region's Bronze and Iron Ages (c.3rd-2nd millennium BC; c.1st millennium BC; Gönster 2014). Along with decorative objects of ivory, bronze, silver,

and gold, they represent the shared status indicators of elites across the competing, connected cultures of their respective ages (Aruz *et al* 2008; 2014).

Since ostriches are not indigenous to Europe, decorated eggs from Bronze and Iron Age archaeological contexts in Greece, Italy and Spain must have been imported from the Middle East and/or North Africa, where ostriches were indigenous during these periods (Brysbaert 2013). Interpretations of where they came from, how they were traded and who decorated them have relied upon iconographic analysis and comparison with other worked media, but have not been able to point with any certainty to where the eggs originated. While this study does not aim to resolve these questions, it highlights potential avenues to do so.

Five whole examples in the British Museum's collection exemplify the problem (for detailed descriptions and illustrations, see Rathje 1986). They were found in the Isis Tomb, an elite burial at Etruscan Vulci (Italy) c.625-550 BC. Four were carved and painted; one was just painted. Motifs include animals, flora, geometric patterns, soldiers and chariots. All were fashioned into vessels with metal attachments, none of which survive. Scholars have debated whether they were decorated imports (Torelli 1965; Rathje 1986: 400), worked by migrant Phoenician craftsmen in Etruria (Markoe 1992: 78-80), or made by local Etruscan craftsmen cognisant of eastern Mediterranean styles and techniques (Rathje 1986; Napolitano 2007). Their motifs and working methods have been compared with contemporary Levantine and Mesopotamian ivory working (Barnett 1982; Feldman 2014: 13-18; Hermann 2000; Winter 1976a; 1976b; 1982), whereas skilled ostrich egg decorating is associated with both North Africa and the Levant (e.g. Rathje 1986: 400; Savio 2004; Le Meaux 2013). Their origins prior to working remain obscure.

Surprisingly little is known about the *chaîne opératoire* of decorated ostrich eggs in the ancient Mediterranean. Carving sites are unknown, but there has been discussion about whether the eggs were blown before shipping (Phillips 2000: 333; Brysbaert 2013: 250), and how they might have been worked (Evely 1993; Koehl 2006; Kandel 2004: 383; Poplin 1995; Brysbaert 2013: 251-52). Much scholarship equates decorative style with cultural identity, which is tenuous at best given how readily motifs can be copied or adapted (Conkey & Hastorf 1993) and especially challenging for periods when artisans were reliant on royal/elite patronage and known to migrate (or be moved) between regions (Gunter 2009: 4-14; Feldman 2014: 11-41). Above all, the eggs' source location is often left to conjecture (e.g. Bass 1997: 165). Only an analysis of where ostrich eggs were laid, alongside a finer understanding of working techniques and iconography, will enable full evaluation of their *chaîne opératoire,* trade routes, and economic and social values across cultures.

Origin problems: ostrich habitats and habits

The first challenge, when considering the eggs' geographic origins, is the vast area from where they could have been sourced. Ostriches are highly nomadic. Their ancient natural habitats encompassed North Africa, the Levant and wider Middle East (Manlius 2001; Potts 2001; Kingdon 1990; Roots 2006; Rowan & Golden 2009: 24), and supported perhaps two sub-species: the now-extinct *Struthio camelus syriacus* in the Arabian peninsula and the Levant, and *S. c. camelus* across northern Africa (Robinson & Matthee 1999; Freitag & Robinson 1993: fig. 1; Brown *et al.* 1982: 32-33).

Assyrian royal texts mention ostrich exploitation. Ashurnasirpal II's (883-859 BC) Nimrud Banquet Inscription describes the king slaying and trapping numerous elephants, lions, wild bulls and ostriches. The live, captive animals' purpose appears to have been for breeding to stock the palace pleasure gardens (Grayson 1991: 291-92). Since ostriches breed well in captivity, they may also have been exploited for their eggs, feathers, oil, leather and meat, in addition to sport. Ostriches were viewed as dangerous and depicted on seals, terracottas, ivories and vessels lashing out, running at speed or being hunted (Herles 2007: 180-98). Xenophon (*Anabasis* 5.3) noted, 'But no ostrich was captured by anyone, and any horseman who chased one speedily desisted; for it would distance him at once in its flight' (Brownson 1922). Ostrich bones are rarely found in excavated archaeological contexts (Tebes 2014: 182-83), however, suggesting the animals were not a significant food resource. In light of these considerations, any understanding of where the eggs were laid must be derived from the shells themselves.

Background, materials and methods

To assess the potential to identify geographical origin from ancient ostrich eggshell (OES), our study selected those examples from the British Museum that met the following criteria: they were either suitable for destructive analysis or were of an appropriate size for scanning electron microscopy (SEM); they came from sites with plausible access into Mediterranean trade networks; they dated from periods that could provide examples of wild and/or captive birds (fifth to first millennia BC; Figure 1; Table 1). We presumed that earlier examples were derived from wild birds, whereas later examples may have been from captive or wild birds. Strontium, carbon, and oxygen isotope analyses were employed to establish whether the eggs had isotope ratios matching the region in which they were found. Modern eggs from Egypt, Israel, Jordan and Turkey were used to develop the sampling methodology, assess elemental concentrations to establish minimum sampling masses for strontium isotope analysis, and allowed multiple samples to be tested to ensure variation across each eggshell matrix was minimal.

We aimed to assess decorating techniques, if we could successfully assign OES to a geographic/climatic region, and whether the ovulating bird was wild or captive. Isotopic

indicators have been established to determine the ecology and climate where an egg was laid and distinguish wild from captive for South African species (Johnson *et al.* 1998). Such methodologies have never been applied to Mediterranean species, or in conjunction with assessment of decorating techniques. Therefore, isotopic analyses, digital microscopy, and SEM were employed.

Isotopic Analyses

OES comprises ~95% inorganic calcite ($CaCO_3$) formed from the food and water ingested by the female bird immediately prior to egg laying and osteoclastic destruction of medullary bone. OES therefore has the potential to act as a palaeoenvironmental proxy and provide evidence of the residential habitat of the adult female bird through combined analyses of strontium ($^{87}Sr/^{86}Sr$), oxygen ($\delta^{18}O$) and carbon ($\delta^{13}C$) isotope ratios (von Schirnding *et al.* 1982; Blum *et al.* 2000). Nitrogen isotopes are also a potentially useful dietary proxy in OES but required too great a mass (c. 50 mg) to be removed from museum objects.

Strontium isotopes in OES derive from the underlying geology, via water, grit and vegetation consumed (Capo *et al.* 1998; Buzon *et al.* 2007; Hartman & Richards 2014). Oxygen isotopes vary geographically in precipitation and groundwaters with climate, latitude, altitude and distance from the coast (Bowen & Wilkinson 2002). The expected oxygen isotope range of modern mean annual precipitation and aridity at each of the findspots (Table 1) is assumed not to differ significantly enough in a relative manner from ancient values to be of concern to this study, e.g. the difference between arid and temperate regions within the study area. All sites examined date to the Holocene and none to the 4.2ky climate event of increased aridity (Bini *et al.* 2019). Nonetheless, given the vast temporal and spatial spread of the OES samples in this study, and the recognised regional heterogeneity in aridity and temperature throughout the Holocene (Finne *et al.* 2019), palaeoclimate reconstruction was outside the scope of this study. This is particularly so because whilst the oxygen isotope ratios of body tissues in a range of animal species, including modern farmed ostriches, have been shown to correlate closely with those of their drinking water, no correlation was found for wild ostriches (Kohn 1996; Johnson *et al.* 1998). Wild ostriches are non-obligate drinkers, tolerant of high aridity and can raise their body temperature to conserve water (Cooper *et al.* 2010). As a consequence, they can hydrate through plant-leaf water; thus the oxygen isotope ratio of OES may reflect that of the plants consumed by the female whilst ovulating, rather than local water sources. The oxygen isotope ratio of plant-leaf water and plant carbon isotope ratios are positively correlated with temperature and aridity, however, and are thus regarded together as proxies for climate change over time or movement between different climatic zones (Johnson *et al.* 1998; Kohn *et al.* 2010; Hartman & Danin 2010).

Carbon isotope ratios of animal tissues will also record the differential consumption of C_3 and C_4 plants, both of which grow in the study region, and thus OES carbon isotope ratios reflect both diet and environment (Johnson *et al.* 1998). It is not thought that ingested rock carbonate contributes to the calcite of OES (von Schirnding *et al.* 1982). Modern ostriches are considered indiscriminate feeders, eating C_3 and C_4 plants, the latter of which are mostly grasses adapted to conditions of drought, high temperature and low fertility; they will also eat succulents (CAM plants), which use both C_3 and C_4 photosynthetic pathways (von Schirnding *et al.* 1982).

Used together, at a range of sites, these isotope systems thus offer the potential to investigate individual variation in OES, and to characterise possible origins based on diet, geology and climate. We conducted strontium isotope and concentration analyses along with oxygen and carbon isotope analyses on 40 c. 1-2mg samples of ancient OES from eleven sites and five modern farmed eggs from the study region (Table 1). The methods are detailed in the Supplementary Information and data tabulated in Table S1 (modern) and Table S2 (archaeological).

Optical Microscopy and SEM

Ten ancient decorated OES examples were assessed for tool marks and working techniques with a Leica MZ APO optical microscope at magnifications from x10 to x250. Five of these were also examined in a Hitachi S3700N variable pressure scanning electron microscope (VP SEM), with inorganic pigments analysed via energy-dispersive X-ray spectroscopy (SEM-EDX). For SEM, the VP mode enables the observation of non-conductive specimens without the need for coating, vital for most museum objects. All specimens were examined with 40P chamber pressure, which was used to eliminate surface charging on (non-conducting) OES. Each specimen was placed on an aluminium SEM stub for examination and imaging using the backscatter electron detector, mostly with an accelerating voltage of 15 kV. Modern reference OES and some experimentally-modified OES fragments were also examined. For the modern OES, the accelerating voltage was often lowered to 10 kV, on account of the fresh condition of the specimens. For optimal visualisation of detail, the working distance varied from 38.5 mm to 12 mm. The magnification ranged from x12 to x500 depending on the fragment under examination. The data-bar on each SEM image records the operating details and the scale bar (microns or mm). Although this model of SEM has a large chamber that can accommodate samples up to 300 mm in diameter, and samples as tall as 110 mm, whole (ancient) decorated ostrich eggs could not be rotated safely within the chamber space to enable the decorative features to be examined or imaged. These were studied using the optical microscope. For the experimental fragments, we used steel tools, flint, bone, and antler to make incision marks, and we buffed, smoothed and abraded using pumice and cuttlefish bone.

Results and Discussion

Where was an egg laid?

A fuller discussion of the data is in the Supplementary Information but key findings are summarised below. Much of the study region's underlying geology consists of limestone, calcareous sandstone and basalt (Table 1) but in many areas the bedrock is overlain by aeolian sediments, removing the connection between the bedrock geology and biosphere strontium. Thus, despite different bedrock at the sites from which OES were recovered, the small range of strontium isotopes (most are within 0.7080-0.7085) were consistent with sediments derived from limestones and calcareous sandstones (Figure 2). The strontium isotope ratios also correlated with previous studies of plants, animals and humans (see Supplementary).

Sites with multiple OES offered our best opportunity to identify eggs originating from different sources. One OES from Amara West, Sudan (988) had a significantly higher strontium isotope ratio than other eggs excavated at the site, whereas one OES from Ur, Iraq (973) had a particularly low ratio comparatively. This suggests these eggs were laid by birds living in different geological and hence geographical environments than for the other OES at the same sites (Figure 2).

In contrast, the carbon and oxygen isotope data vary widely and are strongly correlated (r^2 = 0.61). Despite the large temporal and spatial range of the OES, they cluster into two groups: Group 1, characterised by OES from dry and semi-arid environments with predominantly C_3 plant consumption, and Group 2, by OES from arid and hyper-arid environments and C_4 plant consumption (Figure 3). There is no correlation between the date of the OES and oxygen isotope ratios (r^2 = -0.13). Further statistical analysis is problematic at this stage given the small number of OES from each site and climatic zone in this pilot study, the physiology of the ostrich, and the wide temporal and geographical range. However, for sites with multiple samples, outliers were identified (Ur 973; A'Ali 968; Naukratis 993), suggesting the female was elsewhere during egg laying. OES excavated from regions where ostriches were not indigenous (Vulci; Salamis) are not consistent with origins in arid or hyper-arid environments (Figures 1-3) and group with the majority of OES deriving from sites in cooler, semi-arid environments. The OES oxygen isotope ratios appear to be high but for Group 1 are in line with the range (30 to 41‰) obtained by Johnson *et al*. (1998) for wild ostriches in southern Africa regions broadly comparable in temperature and rainfall to sites 1-10 located above 30°N in this study.

Were the eggs gathered from captive or wild birds?

We hoped to address whether the birds were wild or captive through carbon and oxygen isotope evidence relating to diet. We hypothesised highly divergent data could indicate OES were taken from the wild. There was much less variation in the five modern OES than the archaeological OES, which may be a function of the geographically and climatically limited range from which

the farmed eggs were obtained, and possibly the long-distance transport of modern feedstuffs. It was impossible to ascertain a definite pattern in this regard owing to small sample numbers from each site.

Whilst there is a clear correlation in the ancient OES between location, aridity and temperature, this does not extend to the local precipitation values, which are generally too high when converted (Table S2). In contrast, those of the modern OES do map within uncertainty onto precipitation (Table S1). The oxygen isotope ratios of modern wild OES as non-obligate drinkers (unlike farmed birds provided with water, or even humans) varied widely and could not be directly correlated with precipitation due to body-water being primarily obtained from ingested plants (Johnson *et al*. 1998). The high oxygen isotope ratios of the remaining ancient OES therefore also suggest that these birds were not supplied with drinking water and were wild.

It has also been noted that pronounced ridging and grooving of egg surfaces from wild birds may be due to the need for stronger shells and effects of environmental stresses; the surface of farmed eggs is mostly smooth by comparison (Koyama & Tennyson 2016). Using the SEM, fine, intersecting lines were seen on the ancient specimens that appeared unrelated to decorative motifs or smoothing methods (identified separately). Such pronounced lines were not observed on the modern, farmed eggs examined. We would thus suggest that our ancient examples came from wild birds, which has implications for determining the relative value of ostrich eggs in the ancient world.

How was an egg decorated?

Using the Leica MZ APO optical microscope and Hitachi S-3700N VP SEM, we could characterise different working methods used to produce decorative features. Techniques included polishing, smooth scraping, abrading, pecking, scratching, scoring, picking and shaving. Macroscopically visible pigment colours were predominantly red and black. Examples analysed using SEM-EDX include red ochre (identifiable because of the presence of iron) and carbon, respectively.

Ostrich egg morphology consists of an external surface crystal layer; a palisade layer, which makes up most of the shell thickness; a cone layer towards the interior surface; and an organic membrane that covers the inner surface itself (Figure 4). Texier *et al.* (2010) have drawn attention to three factors that significantly influence the morphology of decorative features on ancient OES:

1. the heterogeneous orientation of the crystalline calcite that makes up 96% of the structure (Richards *et al.* 2000; Feng *et al.* 2001);

2. three different layers in OES, varying in structure and in thickness, which can be affected by thermal changes (Heredia *et al.* 2005);
3. different tool types and materials used for incising or engraving.

Many of the technological features described by Texier *et al.* (2010) on engraved OES container fragments dating to circa 60,000 years ago were seen on the examples under discussion here. Such similarities in technological and decorative modifications (despite great chronological differences in the respective artefact assemblages) lend weight to the assertion that OES structure is the principal determinant of decorative morphology, but the nature and manner of the tool used, is also crucial.

On ancient examples of decorated eggs, superficial incisions usually exhibit a V-shaped profile and do not penetrate beyond the external layer. Deeper incisions with a U-shaped profile penetrate the palisade layer (Figure 5). Our experimental modifications were able to replicate only some of the methods that were macro- and microscopically visible. Tools of different materials produced variations in these profiles according to the angle of the use of the tool, effort expended in creating the incisions, pecking, preparatory buffing or abrading of the surface, and post-incision smoothing of the decorated motifs or incised lines. Our superficial incisions in the outer surface of modern ostrich eggshell exhibited a similar V-shaped profile, while deeper incisions that penetrated the palisade layer had a U-shaped profile (Figure 6). We were also able to recreate scuffing or judder marks observed on ancient examples (Figure 7); these presumably represent areas where minor imperfections in the surface have interrupted the action of the tool in the user's hand.

Variations in the quality of incision were related to the tool material type, angle of application, effort expended and the amount of preparatory or post-carving buffing, abrading or smoothing applied. We were unable to replicate the range of technical skill displayed in the decorated archaeological examples (e.g. Nineveh: Figure 8; Naukratis: Figure 9), and in some cases (e.g. Neolithic Bir Kiseiba: Figure 10) we were unable to suggest by what methods the polishing was achieved or with what tools. Further studies of experimentally-modified modern ostrich eggshell will need to explore the scope and complexity of incision marks created by tools of different materials (including metal, flint, bone, antler and wood), sometimes in conjunction with buffing, smoothing or abrading with organic materials (which occasionally encroaches into the respiratory pores). Overall, the unexpected and considerable variability observed did not correlate conclusively with egg findspots but this was limited by the size of the dataset examined. Our experimental work and the ancient examples examined highlight the diversity and variability of egg carving techniques and how highly skilled the ancient craftworkers were. More data is required to ascertain if certain techniques and decorative motifs can be associated with eggs from particular findspots. Comparison of any such patterns with

isotopically-determined egg origin may help unpick questions such as where or when an egg was decorated within the trade process.

Conclusions

This study has outlined the potential of isotopic analysis and digital microscopy for establishing the regional geographic origins of decorated ostrich eggs and the techniques used to carve them. The results suggest that both avenues of analysis are promising steps towards establishing a deeper understanding of the *chaîne opératoire* for this class of recognised luxuries desired by competing Mediterranean cultures (e.g. Hodos 2009). The results, however, indicate that more work needs to be done across many disciplines. The fact that egg sources may have fluctuated between relatively local and more distant locations in both the Bronze and Iron Ages implies that trade networks in these materials were more flexible, opportunistic and extensive than has been considered previously (e.g. Aruz *et al.* 2014: xviii-xix). Our results also suggest eggs were obtained from the wild rather than through managed means. Additional experimental work, more comparative data and further study of decorating techniques are necessary to investigate discernible patterns regarding egg decoration, and potential nest sites. Nevertheless, this project has demonstrated already that the mechanisms of luxury creation, production and trade in exotic organic materials across both the Bronze and Iron Ages in the Mediterranean and Middle East are of unexpected complexity.

Acknowledgements

This research was supported by the Gerda Henkel Foundation, The British Museum, and the University of Bristol. We are grateful to British Museum colleagues for permission to sample; Andrew Meek and Barbara Wills for sample preparation; Hilary Sloane (NIGL) and Jo Peterkin (Durham University) for sample preparation and isotope measurements; Dan Lawrence for climatic discussion; Chris Jones for SEM advice; Antony Simpson for assistance with Figures 4-10; Matthew Collins for preliminary discussions; Joan Cutts for information on egg decoration; Douglas Russell for species distinction clarifications.

REFERENCES

ARUZ, J., K. BENZEL & J. EVANS. 2008. *Beyond Babylon: art, trade, and diplomacy in the second millennium B.C.* New York: Metropolitan Museum of Art.

ARUZ, J., S. GRAFF & Y. RAKIC. 2014. *Assyria to Iberia at the dawn of the Classical Age.* New York: Metropolitan Museum of Art.

ASCH, K. 2005. *GME 5000 geological map of Europe and adjacent areas*. Hannover: BGR.

BARNETT, R.D. 1982. *Ancient ivories in the Middle East*. Jerusalem: Hebrew University of Jerusalem.

BASS, G. 1997. Prolegomena to a study of marine traffic in raw materials to the Aegean during fourteenth and thirteenth centuries BC. In R. Laffineur and P.P. Betancourt, eds. *TEXNH.* 153-176. Liège: Université de Liège, Histoire de l'art archéologie de la Grèce antique.

BINI, M., G. ZANCHETTA, A. PERSOIU, R. CARTIER, A. CATALA, I. CACHO, J.R. DEAN, F. DI RITA, R.N. DRYSDALE, M. FINNE, I. ISOLA, B. JALALI, F. LIRER, D. MAGRI, A. MASI, L. MARKS, A.M. MERCURI, O. PEYRON, L. SADORI, M.-A. SICRE, F. WELC, C. ZIELHOFER & E. BRISSET. 2019. The 4.2 ka BP Event in the Mediterranean region: an overview. *Climate of the Past* 15(2): 555-577.

BLUM, J.D., E.H. TALIAFERRO, M.T. WEISSE & R.T. HOLMES. 2000. Changes in Sr/Ca, Ba/Ca and 87Sr/86Sr ratios between trophic levels in two forest ecosystems in the northeastern USA. *Biogeochemistry* 49: 87-101.

BROWN, L.H., E.K. URBAN & K. NEWMAN. 1982. *The birds of Africa, vol. 1*. London: Academic Press.

BROWNSON, C.L. 1922. *Xenophon*. Cambridge, MA: Harvard University Press.

BOWEN, G.J. & B. WILKINSON. 2002. Spatial distribution of $\delta^{18}O$ in meteoric precipitation. *Geology* 30: 315-318.

BRYSBAERT, A. 2013. 'The chicken or the egg?' Interregional contacts viewed through a technological lens at Late Bronze Age Tiryns, Greece. *Oxford Journal of Archaeology* 32.3: 233-256.

BUZON, M.R., A. SIMONETTI & R.A. CREASER. 2007. Migration in the Nile Valley during the New Kingdom period: a preliminary strontium isotope study. *Journal of Archaeological Science* 34: 1391-1401.

CAPO, R.C., B.W. STEWART & O.A. CHADWICK. 1998. Strontium isotopes as tracers of ecosystem processes: theory and methods. *Geoderma* 82: 197-225.

CONKEY M.W. & C.A. HASTORF (eds.) 1993. *The uses of style in archaeology*. Cambridge: Cambridge University Press.

COOPER, R.G., J.O. HORBANCZUK, R. VILLEGAS-VIZCAINO, S.K. SEBEI, A.E.F. MOHAMMED & K.M.A. MAHROSE. 2010. Wild ostrich (Struthio camelus) ecology and physiology. *Tropical animal health and production* 42: 363-373.

DERRY, D.R. 1980. *A concise world atlas of geology and mineral deposits*. London: Mining Journal Books Ltd.

EVELY, D. 1993. *Minoan crafts*. Göteborg: Aström.

FENG, Q.L., X. ZHU, H.D. LI & T.N. KIM. 2001. Crystal orientation regulation in ostrich eggshells. *Journal of Crystal Growth* 233: 548-554.

FELDMAN, M.H. 2014. *Communities of style*. Chicago: Chicago University Press.

FINNE, M., J. WOODBRIDGE, I. LABUHN & C.N. ROBERTS. 2019. Holocene hydro-climatic variability in the Mediterranean: A synthetic multi-proxy reconstruction. *Holocene* 29(5): 847-863.

FREITAG, S. & T.J. ROBINSON. 1993. Phylogeographic patterns in mitochondrial DNA of the ostrich (*Struthio camelus*). *The Auk* 110.3: 614-622.

GÖNSTER, Y. 2014. Straußeneier in Bewegung. Ein Indikator für Kulturkontakte im Mittelmeerraum? *Frankfurter elektronische Rundschau zur Altertumskunde* 23: 1-19.

GRAYSON A.K. 1991. *Assyrian rulers of the early first millennia BC I (1114-859 BC.* Royal Inscriptions of the Neo-Assyrian Period, Volume 2. Toronto: University of Toronto Press.

GUNTER, A. 2009. *Greek Art and the Orient*. Cambridge: Cambridge University Press.

HARTMAN, G. & A. DANIN. 2010. Isotopic values of plants in relation to water availability in the Eastern Mediterranean region. *Oecologia* 162: 837-852.

HARTMAN, G. & M. RICHARDS. 2014. Mapping and defining sources of variability in bioavailable strontium isotope ratios in the Eastern Mediterranean. *Geochimica Et Cosmochimica Acta* 126: 250–264.

HEREDIA, A., A.G. RODRÍGUEZ-HERNÁNDEZ, L.F. LOZANO, M.A. PEÑA-RICO, R. VELÁZQUEZ, V.A. BASIUKA & L. BUCIO. 2005. Microstructure and thermal change of texture of calcite crystal in ostrich eggshell. *Struthio camelus*. *Materials Science and Engineering C* 25:1-9.

HERLES M. 2007. Der Vogel Strauß in den Kulturen Altvorderasiens. *Mitteilungen der Deutschen Orient-Gesellschaft zu Berlin* 139: 173-212.

HERMANN, G. 2000. Ivory carving of the first millennium: workshops, traditions and diffusion. In C. Uehlinger, ed. *Images as media*. 267-87. Fribourg: University Press.

HODOS, T. 2009. Colonial engagements in the global Mediterranean Iron Age. *Cambridge Archaeological Journal* 19.2: 221-241.

IAEA. 2001. GNIP Maps and Animations. Vienna: International Atomic Energy Agency. Accessible at http://isohis.iaea.org.

JOHNSON, B.J., M.L. FOGEL & G.H. MILLER. 1998. Stable isotopes in modern ostrich eggshell: a calibration for paleoenvironmental applications in semi-arid regions of southern Africa. *Geochimica et Cosmochimica Acta* 62.14: 2451-2461.

KANDEL, A.W. 2004. Modification of ostrich eggs by carnivores and its bearing on the interpretation of archaeological and paleontological finds. *Journal of Archaeological Science* 31: 377-391.

KINGDON, J. 1990. *Arabian mammals*. New York: Academic Press.

KOEHL, R.B. 2006. *Aegean Bronze Age rhyta*. Philadelphia: INSTAP Academic Press.

KOHN, M.J. 1996. Predicting animal delta O-18: Accounting for diet and physiological adaptation. *Geochimica et Cosmochimica Acta* 60: 4811-4829.

KOHN, M.J. 2010. Carbon isotope compositions of terrestrial C3 plants as indicators of (paleo)ecology and (paleo)climate. *Papers of the National Academic of Sciences of the United States of America* 107: 19691-19695.

LE MEAUX, H. 2013. Des ivoires et des oeufs. *Mélanges de la Casa de Velázquez* 43.1: 85-110.

MANLIUS, N. 2001. The ostrich in Egypt: past and present. *Journal of Biogeography* 28.4: 945-953.

MARKOE, G.E. 1992. In pursuit of metal: Phoenicians and Greeks in Italy. In G. Kopcke and I. Tokumaru, eds. *Greece between East and West, 10th-8th centuries BC*. 61-84. Mainz: Verlag Philipp von Zabern.

NAPOLITANO, F. 2007. Considerations on the making and use of colours in Etruria during the Middle Orientalising period. *Etruscan Studies* 10: 11-25.

PHILLIPS, J. 2000. Ostrich eggshells. In P.T. Nicholson and I. Shaw, eds. *Ancient Egyptian materials and technology*. 332-33. Cambridge: Cambridge University Press.

POPLIN, F. 1995. Sur le polissage des oeufs d'autruche en archéologie. In H. Buitenhuis and H.-P. Uerpmann, eds. *Archaeozoology of the Near East*, vol. 2. 126-139. Leiden: Backhuys.

POTTS, D. 2001. Ostrich distribution and exploitation in the Arabian peninsula. *Antiquity* 75: 182-190.

RATHJE, A. 1986. Five ostrich eggs from Vulci. In J. Swaddling (ed.), *Italian Iron Age artefacts in the British Museum*. 397-404. London: British Museum Press.

RICHARDS, P.D.G., P.A. RICHARDS & M.E. LEE. 2000. Ultrastructural characteristics of ostrich eggshell: outer shell membrane and the calcified layers. *Journal of the South African Veterinary Association* 71: 97-102.

ROBINSON, T.J. & C.A. MATTHEE. 1999. Molecular genetic relationships of the extinct ostrich, *Struthio camelus syriacus*: consequences for ostrich introductions into Saudi Arabia. *Animal Conservation* 2.3: 165-171.

ROOTS, C. 2006. *Flightless birds.* Westport: Greenwood Press.

ROWAN, Y.M. & J. GOLDEN. 2009. The Chalcolithic period of the Southern Levant: a synthetic review. *Journal of World Prehistory* 22: 1-92.

SAVIO, G. 2004. *Le uova di struzzo dipinte nella cultura Punica*. Madrid: Real Academia de la Historia.

TEBES, J.M. 2014. The symbolic and social world of the Quarrayyah pottery iconography. In J.M. Tebes, ed. *Unearthing the wilderness*. 163-202. Leuven: Peeters.

TEXIER, P.J., G. PORRAZ, J. PARKINGTON, J.-P. RIGAUD, C. POGGENPOEL, C. MILLER, C. TRIBOLO, C.R. CARWRIGHT, A. COUDENNEAU, R. KLEIN, T. STEELE, & C. VERNA. 2010. A Howiesons Poort tradition of engraving ostrich eggshell containers dated to 60,000 years ago at Diepkloof Rock Shelter, South Africa. *Papers of the National Academic of Sciences of the United States of America* 107 (14); 6180-6185

TORELLI, M. 1965. Un uovo di struzzo dipinto conservato nel Museo di Tarquinia. *Studi Etruschi* 33: 329-365.

VON SCHIRNDING, Y., N.J. VAN DER MERWE & J.C. VOGEL. 1982. Influence of diet and age on carbon isotope ratios in ostrich eggshell. *Archaeometry* 24: 3-20.

WINTER, I. 1976a. Carved ivory furniture panels from Nimrud: a coherent subgroup of the North Syrian style. *Metropolitan Museum Journal* 11: 25-54.

WINTER, I. 1976b. Phoenician and North Syrian ivory carving in historical context: questions of style and distribution. *Iraq* 38: 1-22.

WINTER, I. 1982. Is there a South Syrian style of ivory carving in the early first millennium BC? *Iraq* 43: 101-130.

FIGURE CAPTIONS

Table 1: List of sites with underlying geology (Asch 2005; Derry 1980), modern aridity indices, and $\delta^{18}O$ zones (IAEA 2001).

Figure 1. A map of the sample sites. Numbers 2, 6, 8 and 9 are modern farmed samples.

Figure 2. A plot of strontium and carbon isotope ratios of modern and archaeological OES.

Figure 3. A plot of carbon and oxygen isotopes of modern and archaeological OES. The vertical green line indicates the -27.4‰ lower limit for low-rainfall C_3 zones, i.e. < 800 mm/year, blue line defines the -23‰ absolute upper limit of solely C_3 plant-based diets, (Kohn 2010) and the brown line the lower limit for 100% C_4 diets calculated using a diet-OES offset of -16.2 +/-0.5‰ (Johnson *et al*. 1998).

Figure 4: Variable pressure scanning electron microscope (VP SEM) image of a cross section of modern reference ostrich eggshell showing A: crystal layer (outer surface); B: palisade layer; C: cone layer; D: organic membrane (inner surface). Scale bar 1mm.

Figure 5a-5d: VP SEM images of EA85166; 2010,1001.527 showing details of a triangular OES fragment with wide and narrow scored (incised) lines. Northern Dongola Reach, Site H29 Feature 3; SF 6236. Scale bars in mm.

Figure 6a-6b: VP SEM images of modern reference OES fragment experimentally modified on the outer surface showing incisions of varying depth with V-shaped profiles (marked V) and deeper incisions with a U-shaped profile (marked U) that penetrate into the palisade layer. M shows an incision with features of both profiles. The network surface crazing is a natural feature of the crystalline outer surface of ostrich eggshell. Figure 6a scale bar in microns; Figure 6b scale bar 1mm.

Figure 7a-7b: VP SEM images Figure 7a: K8556 ostrich eggshell fragment from Nineveh (Iron Age) showing some ancient superficial ‘scuffing’ or ‘judder’ marks replicated experimentally within the broad U-shaped incision shown in Figure 7b. Scale bars in microns.

Figure 8a-8e: VP SEM images of K8556 OES fragment from Nineveh (Iron Age) showing well-executed incised decorative shapes in relief as well as lines (with both V- and U-shaped profiles). Some subsequent buffing or polishing of the areas in higher relief may have been carried out to highlight the decoration. Scale bars in microns.

Figure 9a: 1886,0401.1600 fragment of OES with carved decoration on the inner surface. 27th Dynasty, Sanctuary of Apollo, Naukratis, Egypt © The Trustees of the British Museum. Figure 9b-9c: VP SEM images of the inner surface of this OES fragment from Naukratis showing details of the finely-incised decorative motif, which appears to display surface preparation traces (possibly by abrasion or smoothing) of the higher relief areas, and pecking of the surrounding areas in lower relief. Scale bars in mm.

Figure 10a-10d: VP SEM images. Figure 10a-10b: EA81421; 2004,0517.359; fragment of Neolithic OES with widely-incised and contoured decoration on the outer surface, Bir Kiseiba, Egypt. Figure 10c-10d: EA81430; 2004,0517.358; fragment (21) of Neolithic OES from Bir Kiseiba with widely-incised decoration on the outer surface. Scale bars in mm.

Figures 4-8, 9b-c,10 Image: C.R. Cartwright, © The Trustees of the British Museum

Site	Country	Period	Location	Geology	Aridity Class (modern)	$\delta^{18}O$ precipitation zone (‰)
1. Vulci, Isis tomb	Italy	Iron Age (625-600 BC)	Inland	Tertiary/Tertiary volcanic rocks	Humid	-9 to -6
2. Çanakkale	Turkey	Modern	Inland	Quaternary/Cenozoic sediments	Semi-arid/dry sub humid	-9 to -6
3. Salamis	Cyprus	Iron Age (1050 BC -AD 300)	Island	Quaternary sediments/Ophiolites/ Basalt	Semi-arid/dry sub humid	-9 to -6
4. Tell Atchana	Turkey	Bronze Age (1500-1200 BC)	Coastal	Ophiolites/Basalt	Dry sub-humid	-9 to -6
5. Nineveh	Iraq	Iron Age (700-600 BC)	Inland	Quaternary/Cenozoic sediments	Semi-arid/arid	-9 to -6
6. Gal'ed	Israel	Modern	Coastal	Quaternary/Cenozoic sediments	Semi-arid	-9 to -6
7. Naukratis	Egypt	Iron Age (620-500 BC)	Delta	Tertiary/Quaternary sediments	Arid	-6 to -3
8. Alexandria	Egypt	Modern	Delta	Tertiary/Quaternary sediments	Arid	-6 to -3
9. Azraq Wetlands Reserve	Jordan	Modern	Inland	Cenozoic sediments	Hyperarid	-9 to -6
10. Ur	Iraq	Bronze Age (2600-2400 BC)	Coastal	Quaternary sediments	Arid/ Hyperarid	-6 to -3
11. Mostagedda	Egypt	Bronze Age (1650-1550 BC)	Inland	Tertiary/Quaternary sediments	Hyperarid	-6 to -3
12. A'ali	Bahrain	Bronze-Iron Age (c.3000-1000 BC)	Coastal	Quaternary sediments	Arid/ Hyperarid	-2 to +2
13. Bir Kiseiba	Egypt	Neolithic (c. 6000-4000 BC)	Inland	Cretaceous sediments	Hyperarid	-6 to -3
14. Amara West	Sudan	Bronze Age (1500-1070 BC)	Inland	Precambrian Craton	Hyperarid	-6 to -3
15. Northern Dongola Reach	Sudan	Neolithic (c.6000-4000 BC)	Inland	Cretaceous sediments	Hyperarid	-5 to -2

Table 1

Supplementary Information

Materials and Methods

Scanning Electron Microscopy (SEM)

For SEM, the VP mode enabled the observation of non-conductive specimens without the need for coating, vital for most museum objects. All specimens were examined with 40P chamber pressure, which was used to eliminate surface charging on non-conducting ostrich eggshell. Each specimen was placed on an aluminium SEM stub for examination, mostly with an accelerating voltage of 15 kV using the backscatter electron detector. For the modern OES, this was often lowered to 10 kV, on account of the fresh condition of the specimens. For optimal visualisation of detail, the working distance varied from 38.5 mm to 12 mm. The magnification ranged from x12 to x500 as dictated by the individual fragment being examined. This aspect of the study was undertaken in the British Museum's Department of Scientific Research.

Isotope Analysis

All tools and surfaces were cleaned between each sample with a 2% Decon solution to minimize sample contamination. The modern OES were cleaned of debris by removing the crystalline outer layer and membranous inner layer. This was achieved using a diamond dental burr and a hand-held drill. Multiple samples were taken from each modern OES to test the isotopic homogeneity and the strontium concentrations across the shell in order to determine how much OES needed to be removed from archaeological eggs for analysis. Approximately 1-3 mg of modern OES was then placed in a sealed container and transferred to the laboratory facilities at the University of Durham's Department of Earth Sciences for strontium compositional analysis and an additional duplicate set of samples to the NERC Isotope Geosciences Laboratories in Keyworth for oxygen and carbon isotope analysis.

The archaeological OES samples available for analysis were small and ranged from 12 – 44 mg prior to cleaning. All surfaces and debris were removed with a diamond dental burr and a hand-held drill and discarded. Two archaeological OES samples from Naukratis (985) and Ur (982), for which larger than average samples were provided, were then subject to a gentle leaching protocol to attempt to remove any diagenetic strontium prior to preparing the main batch. Samples were leached for 30 minutes at room temperature in MQ H_2O, monitored throughout to ensure the sample did not disintegrate, and the leachate reserved. This was repeated and the leachate again reserved. The strontium isotope ratio of both leaches and the OES sample were then measured. Negligible differences were found (i.e. <0.00016) between the isotope ratio of sequential leachates and the leached OES (Table S2) at both sites, indicating the leached strontium had very similar isotope ratios to that of the OES. Following this,

the archaeological OES samples were subjected to one leach of 30 minutes at room temperature prior to strontium isotope analysis.

Strontium isotope ($^{87}Sr/^{86}Sr$) and concentration (Sr ppm) analysis was conducted at the Durham Geochemistry Centre in the Earth Science Department of Durham University (UK). The OES samples were prepared using the column chemistry methods outlined in Charlier *et al.* (2006). Samples were placed on a hot plate (100°C) overnight to dissolve in 500µl of nitric acid (HNO_3). Each column was loaded with 80µl of Eichrom Sr specific resin which was then cleaned and preconditioned. Two rounds of 250µl 3 N HNO_3 was rinsed through the column to elute waste. Next, two rounds of 200µl MilliQ water (MQ H_2O) was passed through the columns to elute the strontium fraction. Once collected, each sample was acidified to yield a solution of 3% HNO_3 for analysis. The ^{86}Sr beam was measured to determine the strontium concentrations for each sample. The beam intensity determined the dilution factor for each sample so that each would yield a beam size of approximately 20 V ^{88}Sr to match the International Isotopic Reference Material (IRM), NBS987. The strontium samples were analysed using a Neptune Multi-Collector Inductively Coupled Plasma Mass Spectrometry (MC-ICP-MS). An ESI PFA-50 nebulizer and a micro-cyclonic spray chamber were used to introduce the sample. Instrumental mass bias was corrected by using $^{88}Sr/^{86}Sr$ ratio of 8.375209 (reciprocal of $^{86}Sr/^{88}Sr$ ratio of 0.1194) and an exponential law. Isobaric interferences from Kr and Rb on ^{87}Sr and ^{86}Sr were corrected using ^{83}Kr and ^{85}Rb as monitor masses. International reference standard NBS987 was used to do determine reproducibility. The mean $^{87}Sr/^{86}Sr$ ratio and reproducibility for IRM NBS987 was 0.71026 ± 0.000012 (2σ, n = 26).

Oxygen ($\delta^{18}O$) and carbon ($\delta^{13}C$) isotope analyses were conducted at the NERC Isotope Geoscience Facilities at the British Geological Survey (UK). The modern samples were split into two and one set plasma ashed to remove organics and determine if the resulting values differed. The methodology followed was that outlined in Chenery *et al.* (2012, p310). Approximately 1-3mg of clean eggshell sample was placed in glass vials with sealed septa and placed on a Multiprep system (GV Instruments) hot block (90°C). The vials were evacuated, and four drops of anhydrous phosphoric acid were added. The CO_2 resultant was cryogenically collected for 14 minutes. Oxygen ($\delta^{18}O$) and carbon ($\delta^{13}C$) values were measured using a GV IsoPrime dual inlet mass spectrometer and the results reported in parts per thousand (‰). All results were normalized to Vienna Pee Dee Belemnite (VPDB) and an in-house carbonate standard, Keyworth Carrera Marble, and calibrated against certified reference material (NBS19). Carbonate (VPDB) values were converted using the equation of Coplen (1988): ($\delta^{18}O_{VSMOW} = 1.03091 \times \delta^{18}O_{VPDB} + 30.91$). Analytical uncertainty was estimated at ±0.02 ‰ (1σ, n = 24) for $\delta^{13}C$ and for $\delta^{18}O$ ±0.04 ‰ (1σ, n = 24).

Results and Discussion

Data are tabulated in Tables S1 and S2. Multiple samples were taken from each modern OES to test homogeneity and excellent repeatability was found across each egg (Table S1). The $^{87}Sr/^{86}Sr$ isotope ratios range from 0.70742 to 0.70930 (mean: 0.70833, 1σ = 0.00039, n = 44). Strontium concentrations range from 62 to 1251 ppm (mean: 403, 1σ = 230, n = 42). The $\delta^{18}O_{VPDB}$ values range from -6.5 to 17.6 ‰ (mean: 3.0, 1σ = 5.0, n = 44) and $\delta^{13}C_{VPDB}$ samples from -10.9 to 2.5 ‰ (mean: -7.0, 1σ = 3.7, n = 44). Modern carbon isotope data ($\delta^{13}C$) have not been adjusted to account for the Suess Effect and may be ~1.5‰ lower than equivalent archaeological data (Suess 1958; Friedli *et al.* 1986; Marino & McElroy 1991). The modern samples were plasma ashed to remove any organics and this shifted the data marginally more than the experimental error ($\delta^{13}C$, -0.5‰) (Table S1).

With the exception of Anatolia and the Nubian Arabian Craton straddling the Red Sea, the bedrock of the study region is dominated by young sedimentary and igneous rocks, e.g. limestones, calcareous sandstones and basalts, of Mesozoic and Cenozoic age (Derry 1980; Asch 2005). However, many of the sites are within the Saharan or Arabian deserts and the bedrock is overlain by aeolian sediments, which in some regions are many thousands of metres thick, e.g. Rub' al Khali and the Tigris basin in Iraq (Derry 1980). Such drift deposits will sever the link between the bedrock geology and biosphere strontium depending on the source rock of the drift. Despite different bedrock at the sites from which the archaeological OES were recovered (Table 1, main text), they produced a relatively constrained strontium isotope range (0.7074 – 0.7093), with the majority varying very little (i.e. 0.7080 to 0.7085), suggesting that the birds lived in environments with similar underlying rocks or unconsolidated drift such as aeolian sands (Figure 2 main text).

The mean ratios for strontium isotopes in Theban limestones and Nile sediments is reported to be 0.70777 (Burke *et al.* 1982; Touzeau *et al.* 2014). This OES range of strontium isotopes is thus consistent with limestone terrains of varying aridity or age, i.e. between the estimated lowest limestone ratio of ~0.7072 and atmospheric deposition by rain or seawater at ~0.7092 (Burke *et al.* 1982; Capo *et al.* 1998) and is comparable with other studies of plants, animals and humans from across the study region (e.g. Buzon *et al.* 2007; Henderson *et al.* 2009; Bogaard *et al.* 2014; Hartman & Richards 2014). Such ratios may also be consistent with basalt terrains with high rainfall, e.g. > 1500mm per year (Capo *et al.* 1998), which will shift the plant ratio away from the underlying rock towards that of precipitation, thus overlapping with the limestone range, although few of the study sites have sufficient rainfall to make this a feasible interpretation (Table 1 main text). The modern farmed OES also fall within this range, but whilst all the birds were fed a diet of manufactured pellets, we have no information regarding from what or where these were produced.

One archaeological OES from Amara West, Sudan (988) has a strontium isotope ratio too high to originate from a limestone or basalt region and above the local range of 0.7073 to 0.7079 defined by

Buzon *et al.* (2007), while an OES from Ur, Iraq (973) has a particularly low strontium isotope ratio (Figure S1). Both samples are significantly different to other OES found at these two sites. This suggests these were laid by birds living in different geological and hence geographical environments and is strong evidence that the strontium isotope ratios of the OES have not been entirely overlain by that of the burial environment and retain biogenic integrity. The 988 OES from Amara West may be reflecting a contribution from the rocks of the Nubian Arabian Craton, which would have ratios above 0.7092. One possible explanation for the difference between the low ratio of this OES (973) and the others found at Ur derives from work conducted on the central Anatolian plateau. Bogaard *et al.* (2014) found that plants from terraces at Çatalhöyük had strontium isotope ratios below 0.7075 whilst those on alluvial plains were higher. Similar differences may be present in the environment around Ur, but this is not proven. At the two sites with the most samples, Ur and Naukratis, there is some indication that the strontium isotope ranges of OES may be reflecting an increased contribution from rain or seawater to plants ingested by the ostriches in sites closer to the coast, as most OES from Naukratis have higher strontium isotope ratios than examples from Ur (Figures S1 and S2, and Figure 2 main text). A coastal origin in a non-basaltic arid environment, e.g. in North Africa or the Middle East, would also be consistent with the three OES samples (Vulci, Salamis and Tell Atchana) which have very similar isotope characteristics (Sr, O and C) and sit just below the rain/seawater line (Figures S1 and S2). As Vulci and Salamis are assumed to have no native ostrich population, the result for Tell Atchana is the most interesting. At this site, the underlying geology is basaltic but the strontium isotope ratio of the OES analysed does not reflect this. Therefore, despite being near the coast and possibly having a local wild OES supply, the OES analysed from Tell Atchana (966) appears to have been moved to the site from a different (non-basaltic) arid coastal area.

The strontium isotope ratio and concentration of modern OES was found to be variable between but not within eggs, and the concentration varies in the modern OES from c. 70 ppm to over 400 ppm. There is no correlation between the amount of strontium and the isotope ratio of the OES. Some of the archaeological OES (i.e. from Tell Atchana (966), A'Ali (972) and Naukratis (981)) contain significantly more strontium (Figure S1), which may indicate post-mortem uptake by the OES, but further work is needed to establish the upper limits for OES in different environments as the amount of metabolised strontium can vary with external factors such as calcium availability, coastal proximity and aridity (Freestone *et al.* 2003; Montgomery 2010), and none of the modern OES came from arid regions.

In contrast to the strontium isotope results, there is a large range in OES carbon and oxygen isotope ratios, which cluster in two main groups (Figure 3 main text). The archaeological OES are positively correlated ($r^2 = 0.57$) but these data did not correlate with strontium isotopes or concentrations. As carbon and oxygen isotope ratios increase with temperature and aridity (Hartman & Danin 2010; Miller & Fogel 2016), such a correlation is likely to be a proxy indicator of environment and increasing

consumption of C_4 plants in arid and hyper-arid lower latitude environments, i.e. sites 11-15 in this study lying below 30°N. The OES oxygen isotope ratios appear to be high but for Group 1 are in line with the range (30 to 41‰) obtained by Johnson *et al*. (1998) for wild ostriches in regions of southern Africa, which are broadly comparable in temperature and rainfall to sites 1-10 located above 30°N in this study.

Johnson *et al*. (1998) found that the oxygen isotope ratios of modern wild OES, unlike farmed ones, varied widely and could not be used to establish climatic zones probably due to body water being primarily obtained from ingested plant leaf-water rather than directly from precipitation. In this study, whilst there was a general relationship of $\delta^{18}O_{OES}$ with aridity indices and latitude, there was also no direct absolute correlation between measured $\delta^{18}O_{OES}$ and that of mean annual precipitation at the site when the linear regression ($\delta^{18}O_{OES} = 31.8 + 0.65 \times \delta^{18}O_{dw;}$ Johnson *et al*. 1998, p2456) established from modern controlled ostriches was used. Anomalously high values for OES may be expected given they do not integrate annual temperatures and aridity but are mineralised and laid in a few days, usually in the warmer months of the year (Johnson *et al*. 1998).

The majority of OES samples from low latitude hyper-arid and arid sites (11-15) fall into Group 2 in Figure 3 main text) and are consistent with the eggs being laid in a similar environment to which they were found. However, one OES from A'Ali (968) and the sample from Mostagedda (977) fall into Group 1, indicating the female ostrich was consuming an 100% C_3 diet and inhabiting a dry or semi-arid environment. Conversely, one OES sample from Ur (973) falls into Group 2, suggesting it was laid in an arid/hyper- arid and possibly warmer environment (See Figure 3 main text). The strontium isotope data supports this being a transported egg as it is inconsistent with the Quaternary sediments and other OES at Ur: it suggests the female was inhabiting an arid region of limestone or regions of basalt which are found to the west in the Red Sea region in the Nubian Arabian Craton Saudia Arabia, to the east in Iran and to the south UAE (Derry 1980; Asch 2005). The modern eggs are chiefly consistent with Group 1 but some ostriches appear to have consumed a greater proportion of C_4 plants, which may reflect a modern supply of farmed animal feed or the consumption of CAM or C_4 halophyte plants as the modern farm sites are in coastal, delta or wetland locations. C_4 or CAM consumption also appears to have been the case for one OES sample from Naukratis (993) (see Figure 3, main text), in contrast to the other OES found at the site and possibly the two samples from Ur, a coastal site in prehistory, which fall on the green line defining the absolute maximum carbon isotope ratio for exclusively C_3 consumers in hyper-arid environments (Kohn 2010). Naukratis 993 also had the highest strontium isotope ratio of the eggs excavated from this site but it was not sufficiently different to separate it from the group based on strontium isotopes alone. A strong positive correlation between plant carbon isotopes and increasing aridity, for example during the dry season particularly in green plants, has been reported (Hartman & Danin 2014), and it is of note that all the OES in Group 1 fall between the cut-off for C_3 plants in hyper-

arid environments (green line) and that suggested by Kohn (2010) as the lower limit of carbon isotopes for dry (i.e. annual rainfall < 800 mm per year) regions (blue line). There is, therefore, a gradient of decreasing rainfall from the blue to the green line in Figure 3 main text, suggesting OES closer to the blue line, such as OES from Vulci, Naukratis and Nineveh, are from higher rainfall regions than those closest to the green line, such as OES from Ur. This correlates in terms of the region's overall climate and may also be supported by the higher strontium isotope ranges, i.e. closer to rainwater, observed at Naukratis and Nineveh compared to Ur (Figure S3) although these differences are not large: variation in the fourth decimal place may be within herd or flock variability (Towers *et al*. 2017).

There are clear outliers or significant inter-sample variation at several of the study sites in one or more isotope systems (e.g. Figures S3-5) although the very small sample numbers make defining the isotopic ranges for OES at the sites and further statistical exploration problematic. This implies that in regions where eggs could be sourced relatively locally, some were imported from elsewhere. This study has suggested that both isotope analysis and SEM are possible methods for identifying wild versus captive eggs and eggs that have been subject to long-distance trade across different geological zones or across different latitudes in comparison with others, found at the same site that have not moved as far. This has potentially significant implications because previously, when reconstructing the object-lives of these decorated ostrich eggs, we were able only to identify their findspot and speculate about mid-points relating to trade and decorating. Our study has highlighted source fluctuations in both the Bronze and Iron Ages; it is possible the relative values of ostrich eggs were issues affecting the trading of these luxury goods in both periods.

References

ASCH, K. 2005. *GME 5000 Geological map of Europe and adjacent areas*. Hannover: BGR.

BOGAARD, A., HENTON, E., EVANS, J.A., TWISS, K.C., CHARLES, M.P., VAIGLOVA, P. & RUSSELL, N. 2014. Locating land use at Neolithic Catalhoyuk, Turkey: the implications of Sr-87/Sr-86 signatures in plants and sheep tooth sequences. *Archaeometry* 56: 860-877.

BURKE, W.H., DENISON, R.E., HETHERINGTON, E.A., KOEPNICK, R.B., NELSON, H.F. & OTTO, J.B. 1982. Variation of sea-water $^{87}Sr/^{86}Sr$ throughout Phanerozoic time. *Geology* 10: 516-519.

BUZON, M.R., SIMONETTI, A. & CREASER, R.A. 2007. Migration in the Nile Valley during the New Kingdom period: a preliminary strontium isotope study. *Journal of Archaeological Science* 34: 1391-1401.

CAPO, R.C., STEWART, B.W. & CHADWICK, O.A. 1998. Strontium isotopes as tracers of ecosystem processes: theory and methods. *Geoderma* 82: 197-225.

CHARLIER, B.L.A., GINIBRE, C., MORGAN, D., NOWELL, G.M., PEARSON, D.G., DAVIDSON, J.P. & OTTLEY, C.J. 2006. Methods for the microsampling and high-precision analysis of strontium and rubidium isotopes at single crystal scale for petrological and geochronological applications. *Chemical Geology* 232: 114-133.

CHENERY, C., PASHLEY, V., LAMB, A., SLOANE, H. & EVANS, J. 2012. The oxygen isotope relationship between the phosphate and structural carbonate fractions of human bioapatite. *Rapid Communications in Mass Spectrometry* 26: 309-319.

COPLEN, T.B. 1988. Normalization of oxygen and hydrogen isotope data. *Chemical Geology (Isotope Geosciences Section)* 72: 293-297.

COOPER, R.G., HORBANCZUK, J.O., VILLEGAS-VIZCAINO, R., SEBEI, S.K., MOHAMMED, A.E.F. & MAHROSE, K.M.A. 2010. Wild ostrich (Struthio camelus) ecology and physiology. *Tropical Animal Health and Production* 42: 363-373.

DERRY, D.R. 1980. *A concise world atlas of geology and mineral deposits*. London: Mining Journal Books Ltd.

FREESTONE, I.C., LESLIE, K.A., THIRLWALL, M. & GORIN-ROSEN, Y. 2003. Strontium isotopes in the investigation of early glass production: Byzantine and early Islamic glass from the Near East. *Archaeometry* 45: 19-32.

FRIEDLI, H., LOTSCHER, H., OESCHGER, H., SIEGENTHALER, U. & STAUFFER, B. 1986. Ice core record of the C-13/C-12 C ratio of atmospheric CO2 in the past 2 centuries. *Nature* 324: 237-238.

HARTMAN, G. & DANIN, A. 2010. Isotopic values of plants in relation to water availability in the Eastern Mediterranean region. *Oecologia* 162: 837-852.

HARTMAN, G. & RICHARDS, M. 2014. Mapping and defining sources of variability in bioavailable strontium isotope ratios in the Eastern Mediterranean. *Geochimica Et Cosmochimica Acta* 126: 250–264.

HENDERSON, J., EVANS, J. & BARKOUDAH, Y. 2009. The roots of provenance: glass, plants and isotopes in the Islamic Middle East. *Antiquity* 83: 414-429.

JOHNSON, B.J., FOGEL, M.L. & MILLER, G.H. 1998. Stable isotopes in modern ostrich eggshell: a calibration for paleoenvironmental applications in semi-arid regions of southern Africa. *Geochimica et Cosmochimica Acta* 62.14: 2451-2461.

KOHN, M.J. 2010. Carbon isotope compositions of terrestrial C3 plants as indicators of (paleo)ecology and (paleo)climate. *Proceedings of the National Academy of Sciences of the United States of America* 107: 19691-19695.

MARINO, B.D. & MCELROY, M.B. 1991. Isotopic composition of atmospheric CO2 inferred from carbon in C4 plant cellulose. *Nature* 349: 127-131.

MILLER, G.H. & FOGEL, M.L. 2016. Calibrating delta O-18 in Dromaius novaehollandiae (emu) eggshell calcite as a paleo-aridity proxy for the Quaternary of Australia. *Geochimica Et Cosmochimica Acta* 193: 1-13.

MONTGOMERY, J. 2010. Passports from the past: Investigating human dispersals using strontium isotope analysis of tooth enamel. *Annals of Human Biology* 37: 325-346.

SUESS, H.E. 1958. Radioactivity of the atmosphere and hydrosphere. *Annual Review of Nuclear Science* 8: 243-256.

TOUZEAU, A., AMIOT, R., BLICHERT-TOFT, J., FLANDROIS, J.-P., FOUREL, F., GROSSI, V., MARTINEAU, F., RICHARDIN, P. & LECUYER, C. 2014. Diet of ancient Egyptians inferred from stable isotope systematics. *Journal of Archaeological Science* 46: 114-124.

TOWERS, J., BOND, J., EVANS, J., MAINLAND, I. & MONTGOMERY, J. 2017. An isotopic investigation into the origins and husbandry of Mid-Late Bronze Age cattle from Grimes Graves, Norfolk. *Journal of Archaeological Science Reports* 15: 59-72.

VON SCHIRNDING, Y., VAN DER MERWE, N.J. & VOGEL, J.C. 1982. Influence of diet and age on carbon isotope ratios in ostrich eggshell. *Archaeometry* 24: 3-20.

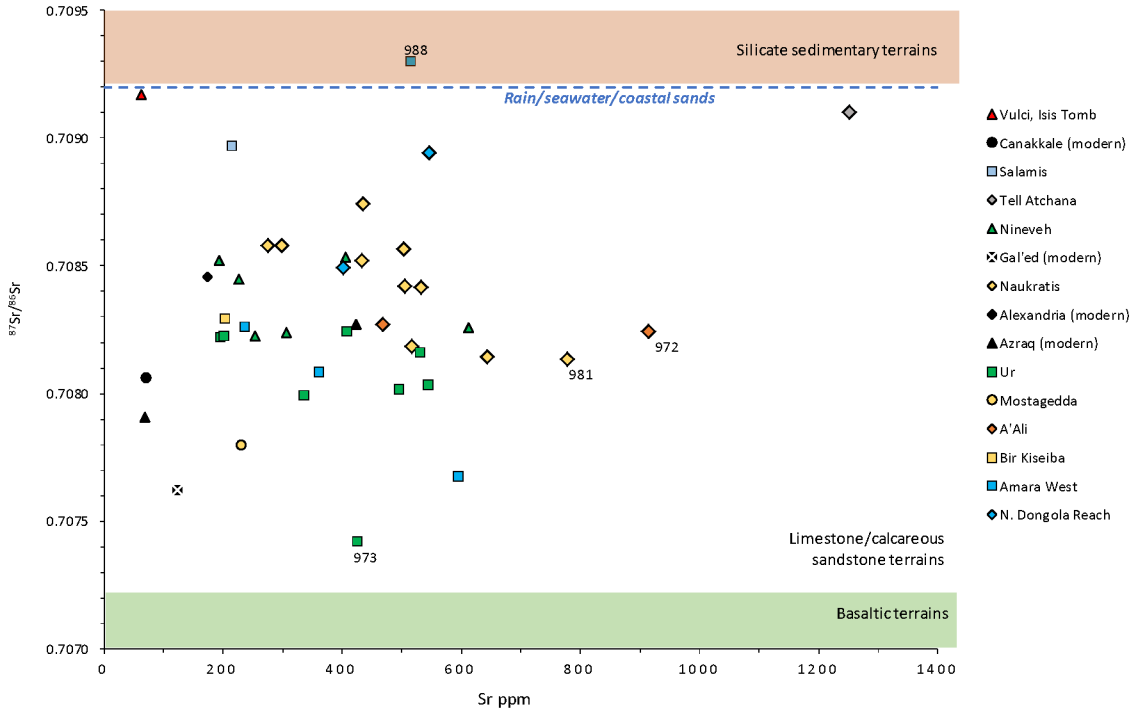

Figure S1. A plot of strontium isotope and concentrations of modern and archaeological OES. The majority of the samples have isotope ratios consistent with limestone and calcareous sandstone regions. 2sd analytical uncertainty is within the symbols.

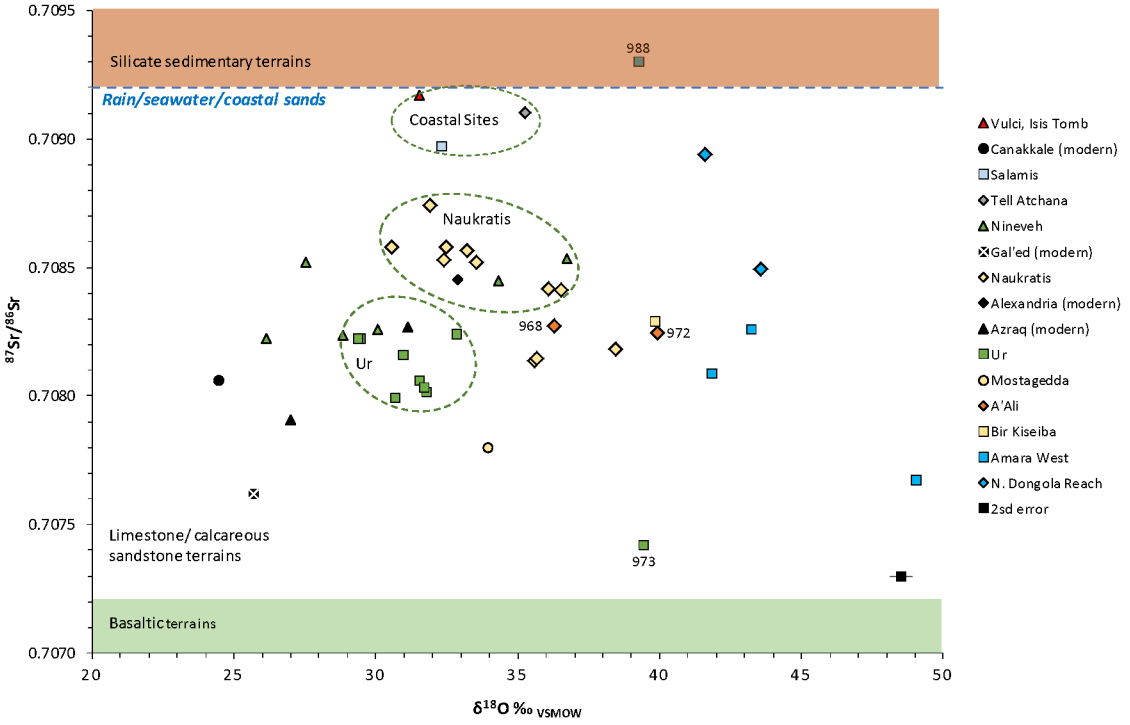

Figure S2. A plot of strontium and oxygen isotope ratios of modern and archaeological OES.

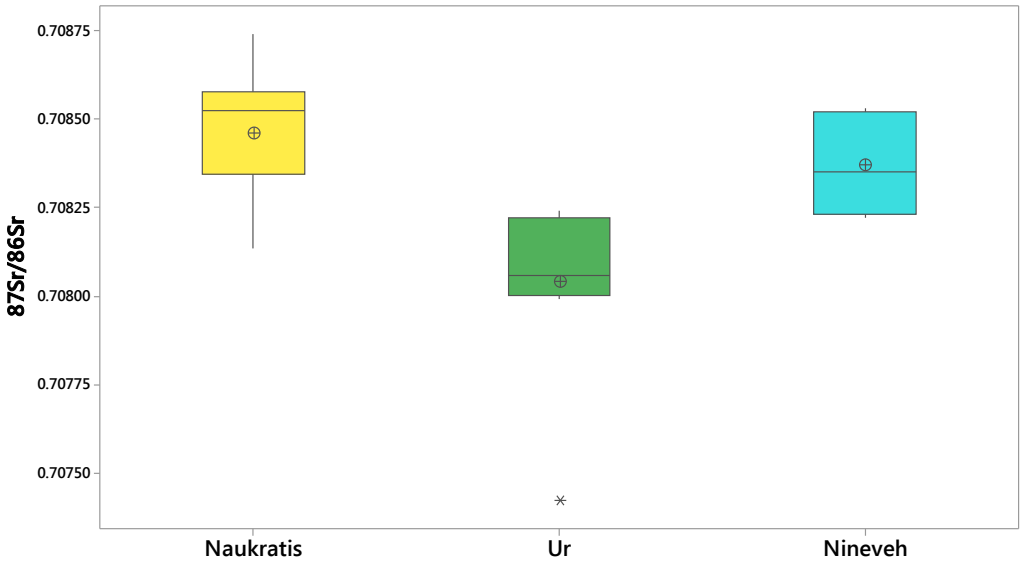

Statistics	Naukratis	Ur	Nineveh
N	10	9	6
Mean	0.70846	0.70804	0.70837
StDev	1.937E-04	2.520E-04	1.462E-04
Minimum	0.70814	0.70742	0.70822
Maximum	0.70874	0.70824	0.70853

Figure S3. Box and whisker plot and descriptive statistics for strontium isotope ratios at the three sites with 6 or more OES samples.

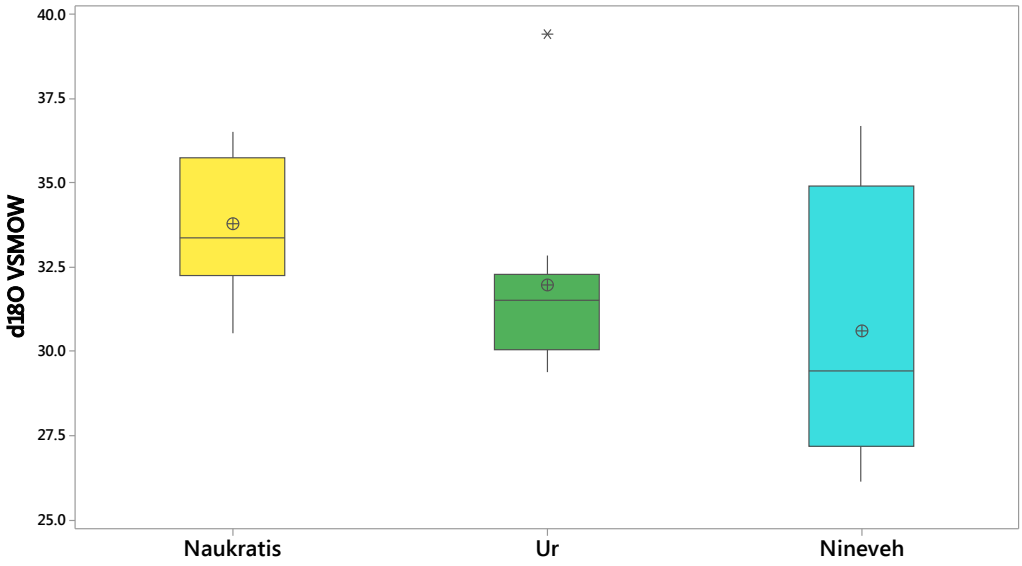

Statistics	Naukratis	Ur	Nineveh
N	10	9	6
Mean	33.799	31.980	30.603
StDev	2.0434	3.0012	4.1009
Minimum	30.550	29.388	26.138
Maximum	36.536	39.413	36.718

Figure S4. Box and whisker plot and descriptive statistics for oxygen isotope ratios at the three sites with 6 or more OES samples.

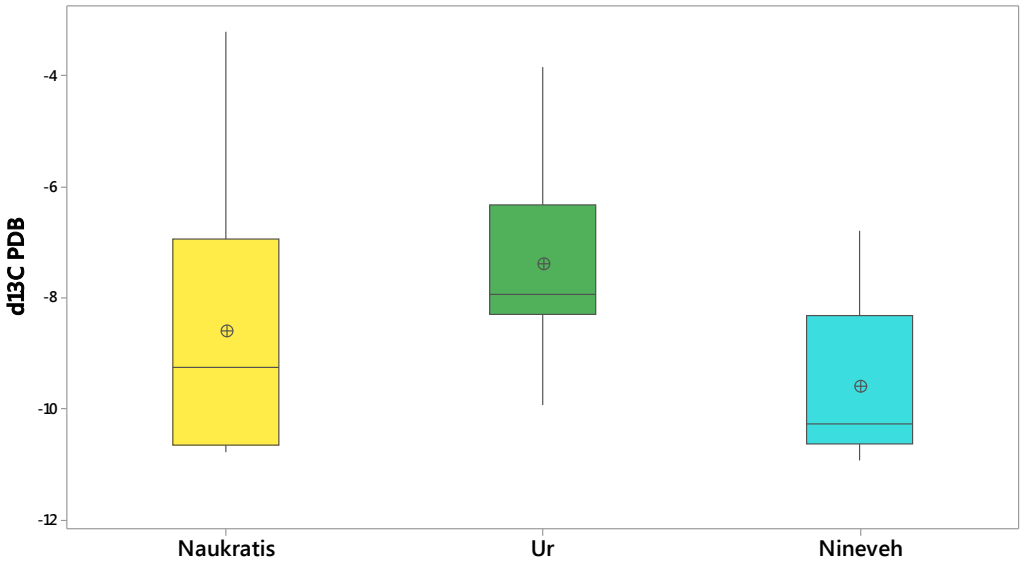

Statistics	Naukratis	Ur	Nineveh
N	10	9	6
Mean	-8.5821	-7.3791	-9.5847
StDev	2.3566	1.7176	1.5505
Minimum	-10.766	-9.9092	-10.915
Maximum	-3.2	-3.8268	-6.7796

Figure S5. Box and whisker plot and descriptive statistics for carbon isotope ratios at the three sites with 6 or more OES samples.

Country	Site	Lab code	n	treatment	$\delta^{13}C_{PDB}$ ‰		$\delta^{13}C_{PDB}$ ‰	$\delta^{18}O_{PDB}$ ‰		$\delta^{18}O_{VSMOW}$ ‰		$\delta^{18}O_{VSMOW}$ ‰	Lab code	n	$^{87}Sr/^{86}Sr$ norm	2SE	Sr ppm
					mean	sd	plant*	mean	sd	mean	sd	drinking water**					
Egypt	Alexandria	784 (a-e)	5	plasma ashed	-3.27	0.12	-19.47	1.67	0.05	32.58	0.05	1.2					
		784 (a-e)	5	unashed	-3.16	0.12	-19.36	1.92	0.07	32.84	0.07	1.6	783 (a,b,c)	3	0.708455	0.000006	173
Israel	Gal'ed	2094 (a-c)	3	unashed	-3.12	0.27	-19.32	-5.07	0.04	25.69	0.04	-9.4	2094a	1	0.707621	0.000013	124
Jordan	Azraq Wetlands Reserve	2095a (1-3)	3	unashed	-4.86	0.02	-21.06	0.21	0.03	31.14	0.03	-1.0	2095a	1	0.708270	0.000008	423
		2095b (1-3)	3	unashed	-9.22	0.04	-25.42	-3.80	0.11	27.00	0.09	-7.4	2095b	1	0.707906	0.000012	69
Turkey	Çanakkale	782 (a-e)	5	plasma ashed	-7.04	0.02	-23.24	-6.53	0.05	24.13	0.06	-11.8					
		782 (a-e)	5	unashed	-6.87	0.04	-23.07	-6.24	0.10	24.43	0.11	-11.3	781 (a,b,c)	3	0.708061	0.000005	70

Table S1. Oxygen, carbon and strontium isotopes and concentration for modern ostrich egg shell. Data are mean values of different samples taken to assess intra-egg homogeneity. Values for plant* $\delta^{13}C$ are calculated using the OES diet-carbonate offset of -16.2‰ reported by von Schirnding *et al*. 1982. Values for drinking water** are calculated using the equation of Johnson *et al*. 1998: $\delta^{18}O_{dw} = 31.8 + 0.65 \times \delta^{18}O_{carb}$. Analytical reproducibility was estimated at: +/- 0.02‰ (1sd) for $\delta^{13}C$; +/- 0.04‰ (1sd) for $\delta^{18}O$; +/-0.000012 (2sd) for $^{87}Sr/^{86}Sr$.

Country	Site	Lab code	British Museum registration numbers	$\delta^{13}C_{PDB}$ ‰	$\delta^{13}C_{PDB}$ ‰	$\delta^{18}O_{PDB}$ ‰	$\delta^{18}O_{VSMOW}$ ‰	$\delta^{18}O_{VSMOW}$ ‰	$^{87}Sr/^{86}Sr$ norm	2SE	Sr ppm
				OES	plant*	OES	OES	drinking water**			
Bahrain	A'Ali	968	1889.1213.11 (136243) (a)	-9.4	-25.6	5.2	36.3	6.9	0.708272	0.000013	468
Bahrain	A'Ali	972	1889.1213.11 (136243 (b)	-1.4	-17.6	8.7	39.9	12.5	0.708244	0.000009	914
Cyprus	Salamis	965	1967.1104.12	-9.2	-25.4	1.4	32.3	0.8	0.708970	0.000011	214
Egypt	Mostagedda	977	Pan grave bead 1930.0711.291 ea63268	-10.3	-26.5	2.9	34.0	3.3	0.707797	0.000011	231
Egypt	Naukratis, Temple of Apollo	979	1888.0601.85 (1)	-10.6	-26.8	2.5	33.5	2.7	0.708521	0.000011	433
Egypt	Naukratis, Temple of Apollo	981	1888.0601.85 (2)	-6.9	-23.1	4.5	35.6	5.9	0.708136	0.000010	778
Egypt	Naukratis, Temple of Apollo	980	1888.0601.85 (3)	-9.4	-25.6	-0.4	30.6	-1.9	0.708581	0.000013	299
Egypt	Naukratis, Temple of Apollo	995	1888.0601.85 (4)	-8.5	-24.7	1.5	32.5	1.0	0.708582	0.000010	275
Egypt	Naukratis, Temple of Apollo	987	1888.0601.85 (5)	-10.6	-26.8	2.2	33.2	2.2	0.708566	0.000009	504
Egypt	Naukratis, Temple of Apollo	993	1888.0601.85 (6)	-3.2	-19.4	1.0	31.9	0.2	0.708743	0.000012	434
Egypt	Naukratis, Temple of Apollo	991	1888.0601.85 (7)	-9.7	-25.9	5.4	36.5	7.3	0.708414	0.000009	533
Egypt	Naukratis, Temple of Apollo	989	1888.0601.85 (8)	-9.1	-25.3	5.0	36.1	6.6	0.708419	0.000008	506
Egypt	Naukratis, Temple of Apollo	986	1888.0601.85 (9)	-6.9	-23.1	4.6	35.7	5.9	0.708145	0.000008	643
Egypt	Naukratis, Temple of Apollo	985	1888.0601.85a G&R	-10.8	-27.0	1.4	32.4	0.9	0.708530	0.000005	**n.d.**
		985	leachate 1						0.708461	0.000007	
		985	leachate 2						0.708373	0.000007	

Country	Site	Lab code	British Museum registration numbers	$\delta^{13}C_{PDB}$ ‰	$\delta^{13}C_{PDB}$ ‰	$\delta^{18}O_{PDB}$ ‰	$\delta^{18}O_{VSMOW}$ ‰	$\delta^{18}O_{VSMOW}$ ‰	$^{87}Sr/^{86}Sr$ norm	2SE	Sr ppm
				OES	plant*	OES	OES	drinking water**			
Egypt	Naukratis, Temple of Apollo	2092	18,860,401.16	-9.5	-25.7	7.3	38.5	10.2	0.708183	0.000008	516
Egypt	Bir Kiseiba	2093	20,040,517.36	1.6	-14.6	8.7	39.8	12.4	0.708292	0.000015	204
Iraq	Nineveh	975	K8556 BOX 1 WAS 1.8Q (a)	-6.8	-23.0	5.6	36.7	7.6	0.708533	0.000009	407
Iraq	Nineveh	964	K8556 BOX 1 WAS 2.2Q (b)	-10.2	-26.4	3.3	34.3	3.9	0.708449	0.000009	226
Iraq	Nineveh	970	K8556 BOX 1 WAS 2.5Q (C)	-10.9	-27.1	-4.6	26.1	-8.7	0.708224	0.000011	253
Iraq	Nineveh	969	K8556 BOX 2 WAS 1.4 (a)	-8.8	-25.0	-0.8	30.1	-2.7	0.708258	0.000009	613
Iraq	Nineveh	961	K8556 BOX 2 WAS 1.7Q (C)	-10.4	-26.6	-3.3	27.6	-6.5	0.708520	0.000009	193
Iraq	Nineveh	962	K8556 BOX 2 WAS 1.8Q (c)	-10.5	-26.7	-2.0	28.8	-4.6	0.708237	0.000011	307
Iraq	Ur	990	1928.1010.705 (A)	-8.0	-24.2	0.8	31.7	-0.2	0.708034	0.000012	544
Iraq	Ur	984	1928.1010.705 (B)	-8.2	-24.4	0.8	31.8	0.0	0.708018	0.000010	495
Iraq	Ur	983	1928.1010.707 (A)	-9.9	-26.1	1.9	32.9	1.6	0.708243	0.000009	408
Iraq	Ur	982	1928.1010.707(B)	-8.3	-24.5	0.6	31.6	-0.4	0.708061	0.000004	n.d.
		982	leachate 1						0.708060	0.000005	
		982	leachate 2						0.708063	0.000007	
Iraq	Ur	974	1929.1017.497 (a)	-7.6	-23.8	-0.2	30.7	-1.7	0.707992	0.000010	335
Iraq	Ur	963	1929.1017.497 (b)	-7.9	-24.1	0.0	31.0	-1.3	0.708160	0.000012	531

Country	Site	Lab code	British Museum registration numbers	$\delta^{13}C_{PDB}$ ‰	$\delta^{13}C_{PDB}$ ‰	$\delta^{18}O_{PDB}$ ‰	$\delta^{18}O_{VSMOW}$ ‰	$\delta^{18}O_{VSMOW}$ ‰	$^{87}Sr/^{86}Sr$ norm	2SE	Sr ppm
				OES	plant*	OES	OES	drinking water**			
Iraq	Ur	973	1929.1106.7 ea59727	-3.8	-20.0	8.2	39.4	11.7	0.707421	0.000011	425
Iraq	Ur	971	1930.1213.299C (a)	-6.3	-22.5	-1.5	29.4	-3.7	0.708223	0.000010	200
Iraq	Ur	967	130.1213.229C (b)	-6.3	-22.5	-1.4	29.5	-3.6	0.708221	0.000011	195
Italy	Vulci, Isis tomb	2091	18,500,227.90	-10.5	-26.7	0.6	31.5	-0.4	0.709169	0.000010	62
Sudan	Northern Dongola Reach	976	2010.1001.479 EA85118 (BEADX4)	-1.9	-18.1	12.3	43.6	18.1	0.708494	0.000011	401
Sudan	Northern Dongola Reach	978	2010.1001.516 EA85155	-3.0	-19.2	10.3	41.6	15.1	0.708942	0.000010	545
Sudan	Amara West	988	F1111 Amara West	1.1	-15.1	8.1	39.2	11.5	0.709301	0.000007	514
Sudan	Amara West	992	F2288 Amara West	-0.6	-16.8	10.6	41.9	15.5	0.708087	0.000010	361
Sudan	Amara West	994	F9265 Amara West	-1.5	-17.7	11.9	43.2	17.6	0.708262	0.000010	236
Sudan	Amara West	996	F6344 Amara West	2.5	-13.7	17.6	49.0	26.5	0.707675	0.000009	595
Turkey	Tell Atchana	966	1951.0102.160	-8.4	-24.6	4.2	35.3	5.3	0.709101	0.000010	1251

Table S2. Oxygen, carbon and strontium isotopes and concentration for archaeological ostrich egg shell. Samples 982 and 985 are the two samples subjected to leaching to assess diagenetic strontium and the shell data is the value after leaching. Modern OES samples have not been corrected for the Suess (1958) offset. Values for plant* $\delta^{13}C$ are calculated using the OES diet-carbonate offset of -16.2‰ reported by von Schirnding *et al*. 1982. Values for drinking water** are calculated using the equation of Johnson *et al*. 1998: $\delta^{18}O_{dw} = 31.8 + 0.65 \times \delta^{18}O_{carb}$. Analytical reproducibility was estimated at: +/- 0.02‰ (1sd) for $\delta^{13}C$; +/- 0.04‰ (1sd) for $\delta^{18}O$; +/-0.000012 (2sd) for $^{87}Sr/^{86}Sr$.

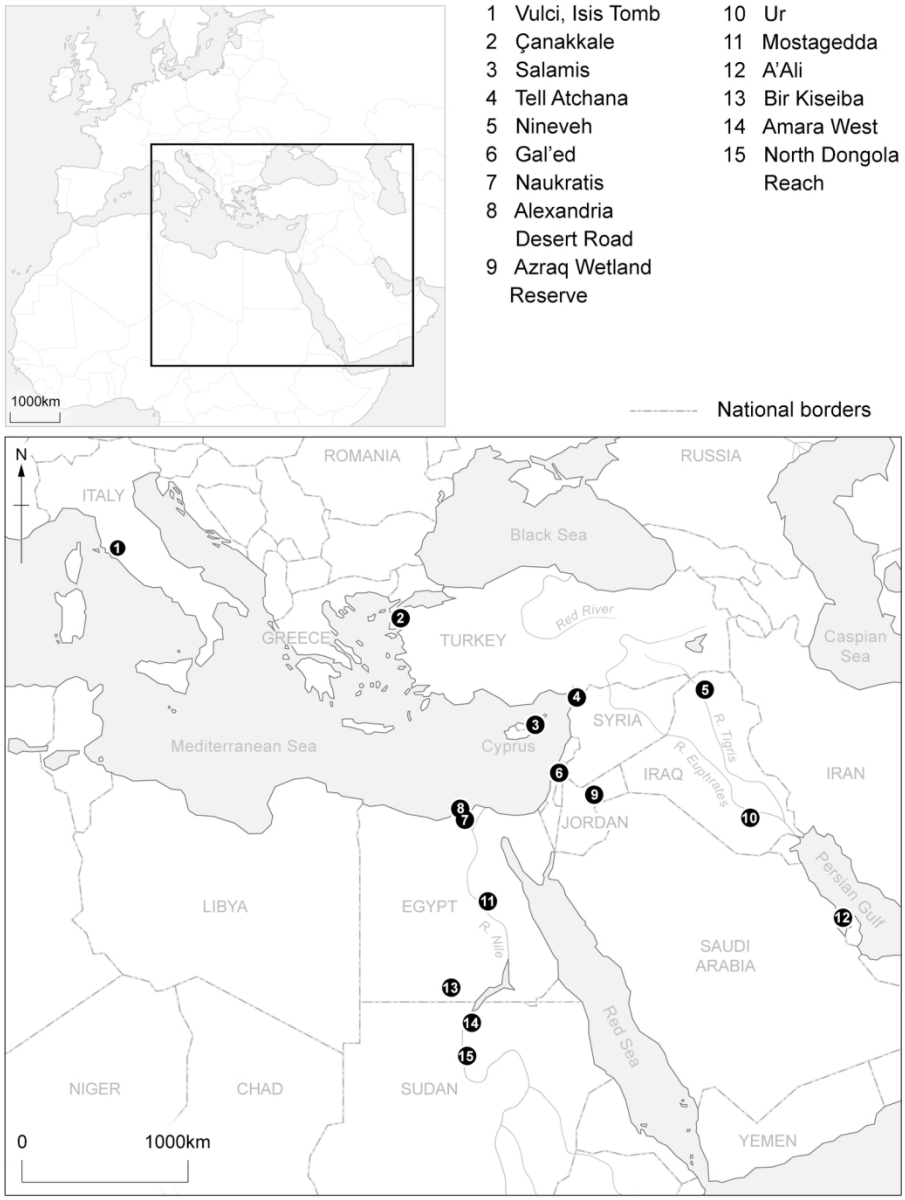

Figure 1. A map of the sample sites. Numbers 2, 6, 8 and 9 are modern farmed samples.

137x180mm (300 x 300 DPI)

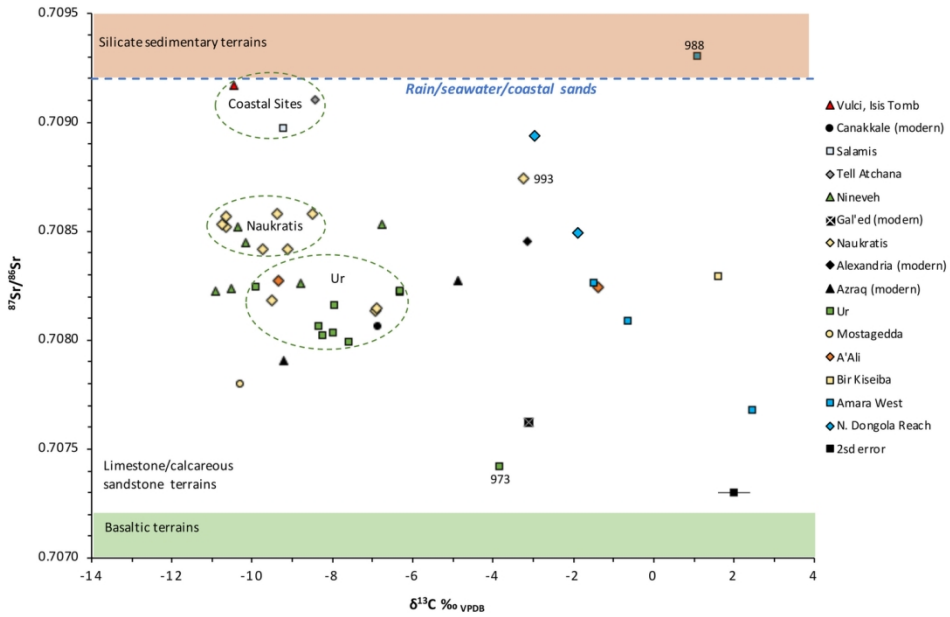

Figure 2. A plot of strontium and carbon isotope ratios of modern and archaeological OES.

135x88mm (300 x 300 DPI)

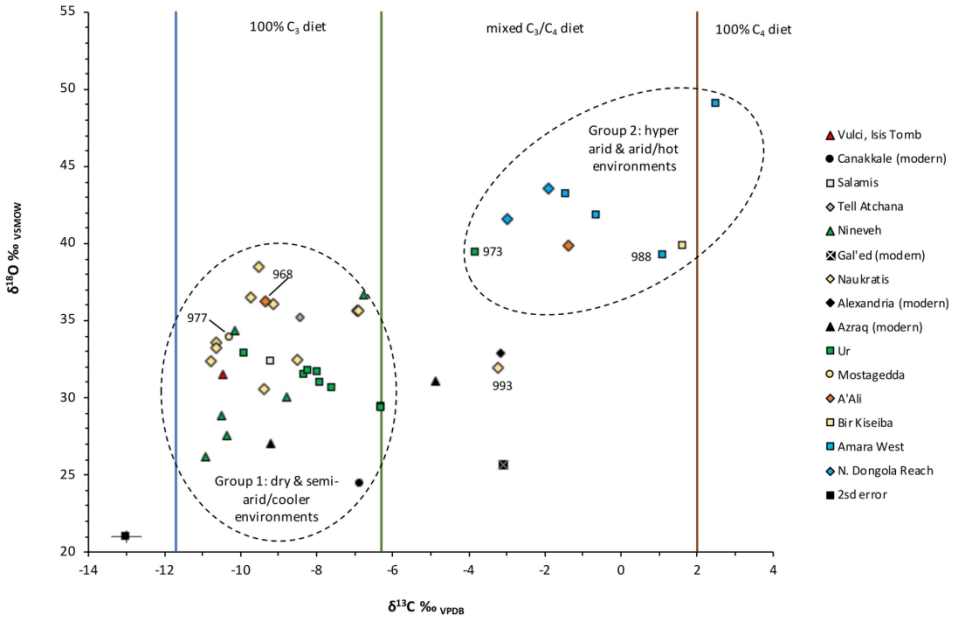

Figure 3. A plot of carbon and oxygen isotopes of modern and archaeological OES. The vertical green line indicates the -27.4‰ lower limit for low-rainfall C3 zones, i.e. < 800 mm/year, blue line defines the -23‰ absolute upper limit of solely C3 plant-based diets, (Kohn 2010) and the brown line the lower limit for 100% C4 diets calculated using a diet-OES offset of -16.2 +/-0.5‰ (Johnson et al. 1998).

165x111mm (300 x 300 DPI)

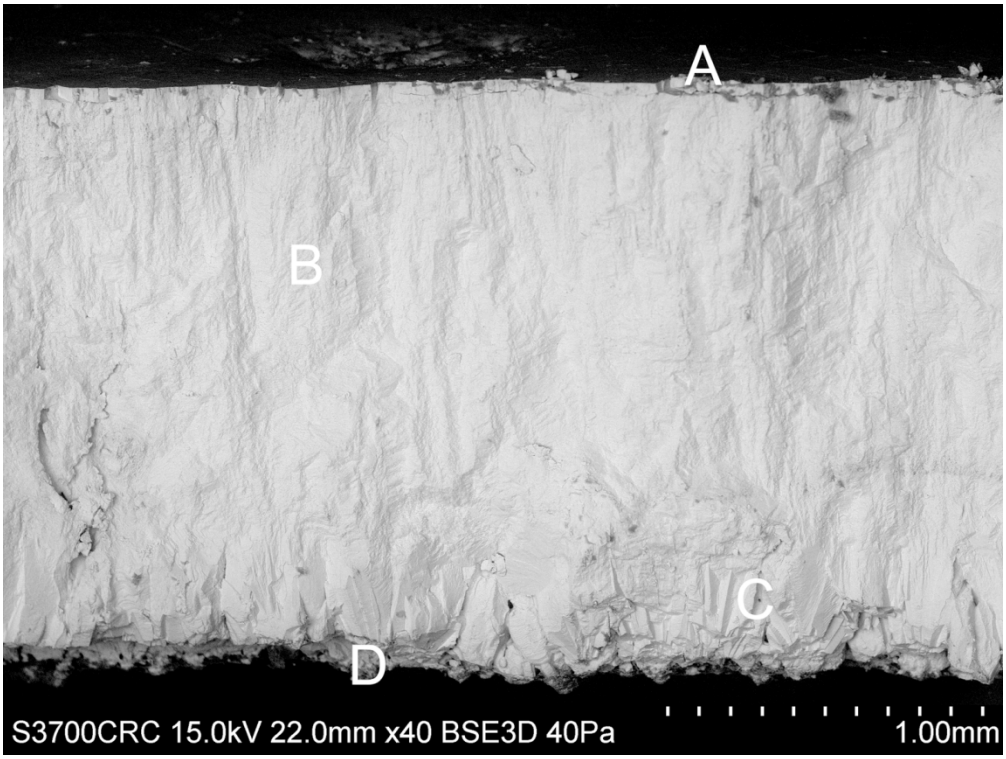

Figure 4: Variable pressure scanning electron microscope (VP SEM) image of a cross section of modern reference ostrich eggshell showing A: crystal layer (outer surface); B: palisade layer; C: cone layer; D: organic membrane (inner surface). Scale bar 1mm.

134x101mm (300 x 300 DPI)

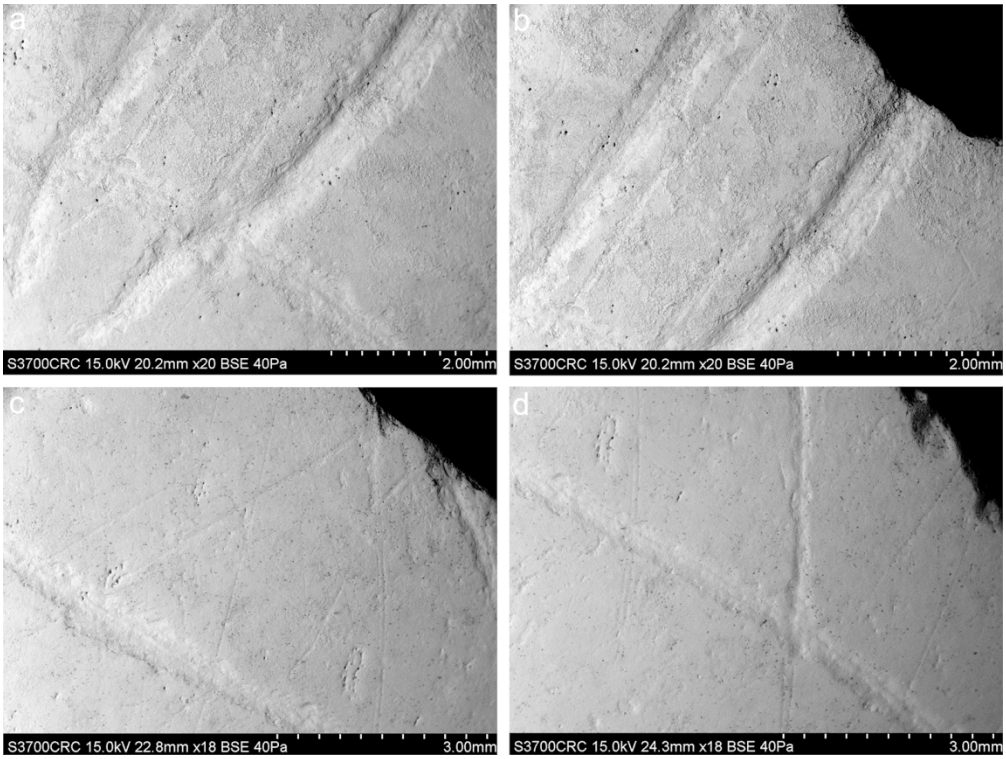

Figure 5a-5d: VP SEM images of EA85166; 2010,1001.527 showing details of a triangular OES fragment with wide and narrow scored (incised) lines. Northern Dongola Reach, Site H29 Feature 3; SF 6236. Scale bars in mm.

134x101mm (300 x 300 DPI)

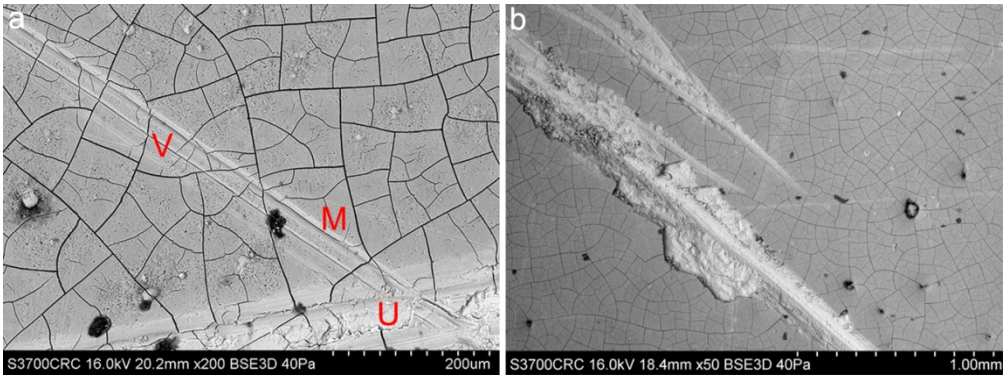

Figure 6a-6b: VP SEM images of modern reference OES fragment experimentally modified on the outer surface showing incisions of varying depth with V-shaped profiles (marked V) and deeper incisions with a U-shaped profile (marked U) that penetrate into the palisade layer. M shows an incision with features of both profiles. The network surface crazing is a natural feature of the crystalline outer surface of ostrich eggshell. Figure 6a scale bar in microns; Figure 6b scale bar 1mm.

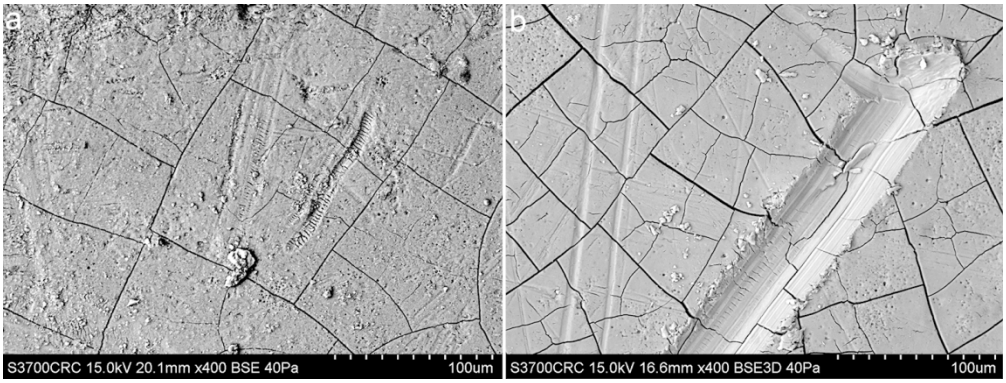

Figure 7a-7b: VP SEM images Figure 7a: K8556 ostrich eggshell fragment from Nineveh (Iron Age) showing some ancient superficial 'scuffing' or 'judder' marks replicated experimentally within the broad U-shaped incision shown in Figure 7b. Scale bars in microns.

134x50mm (300 x 300 DPI)

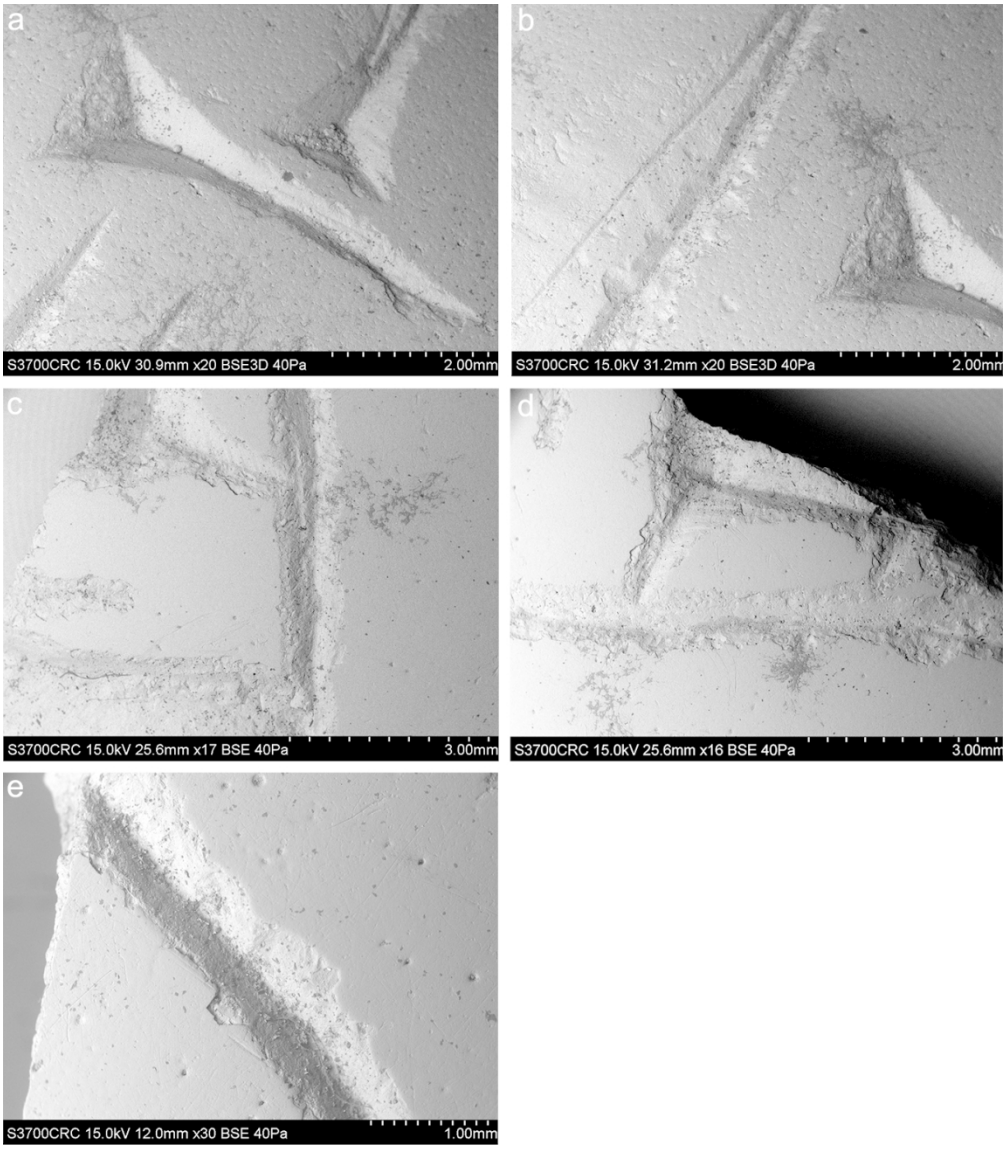

Figure 8a-8e: VP SEM images of K8556 OES fragment from Nineveh (Iron Age) showing well-executed incised decorative shapes in relief as well as lines (with both V- and U-shaped profiles). Some subsequent buffing or polishing of the areas in higher relief may have been carried out to highlight the decoration. Scale bars in microns.

135x153mm (256 x 256 DPI)

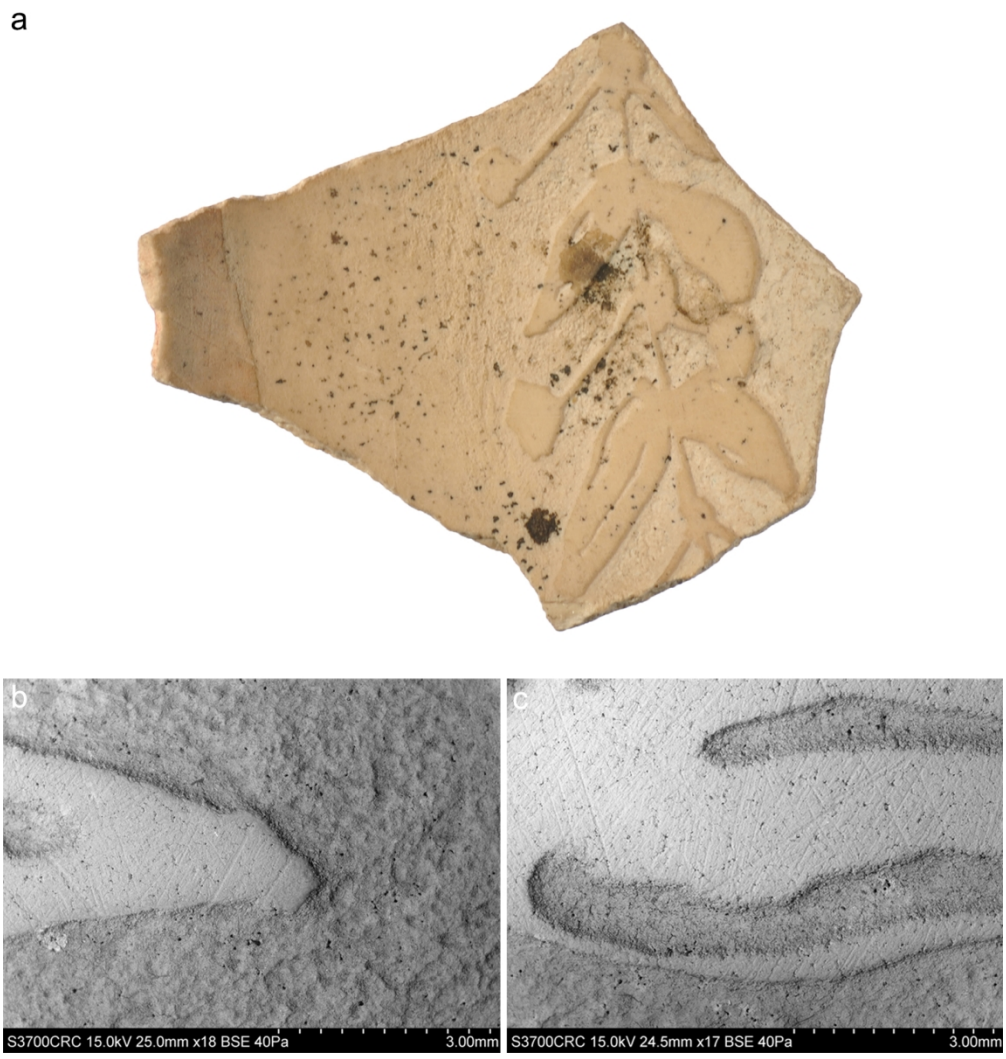

Figure 9a: 1886,0401.1600 fragment of OES with carved decoration on the inner surface. 27th Dynasty, Sanctuary of Apollo, Naukratis, Egypt © The Trustees of the British Museum. Figure 9b-9c: VP SEM images of the inner surface of this OES fragment from Naukratis showing details of the finely-incised decorative motif, which appears to display surface preparation traces (possibly by abrasion or smoothing) of the higher relief areas, and pecking of the surrounding areas in lower relief. Scale bars in mm.

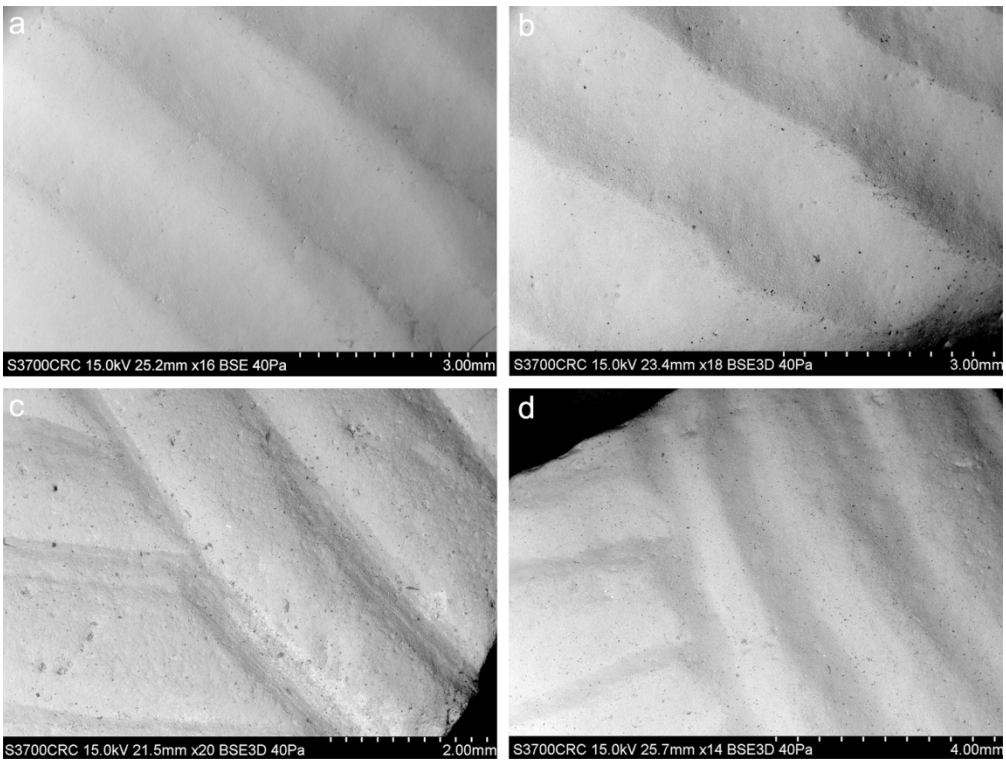

Figure 10a-10d: VP SEM images. Figure 10a-10b: EA81421; 2004,0517.359; fragment of Neolithic OES with widely-incised and contoured decoration on the outer surface, Bir Kiseiba, Egypt. Figure 10c-10d: EA81430; 2004,0517.358; fragment (21) of Neolithic OES from Bir Kiseiba with widely-incised decoration on the outer surface. Scale bars in mm.

134x101mm (300 x 300 DPI)